

TUNABLE PHOSPHORESCENT NIR OXYGEN INDICATORS BASED ON MIXED BENZO- AND NAPHTHO PORPHYRIN COMPLEXES

Fabian Niedermair,^{,†} Sergey M. Borisov,[†] Gunter Zenkl,[†] Oliver T. Hofmann,[‡] Hansjörg Weber,[¥] Robert Saf[§] and Ingo Klimant[†]*

[†] Institute of Analytical Chemistry and Food Chemistry, Graz University of Technology, Stremayrgasse 16, A-8010 Graz, Austria

[‡] Institute of Solid State Physics, Graz University of Technology, Petersgasse 16, A-8010 Graz, Austria

[¥] Institute of Organic Chemistry, Graz University of Technology, Stremayrgasse 16, A-8010 Graz, Austria

[§] Institute for Chemistry and Technology of Materials, Graz University of Technology, Stremayrgasse 16, A-8010 Graz, Austria

Correspondence to: F. Niedermair (E-mail: f.niedermair@tugraz.at)

Supporting Information

Synthesis

Synthesis of the precursor compounds

2H-Isoindole-4,5,6,7-tetrahydro-1-carboxylic acid ethyl ester. A similar procedure to the work of Borek et al. was applied.¹ 1-Nitrocyclohexene (2.66 mL, 3.0 g, 23.6 mmol, 1.0 eq.) and ethyl isocynoacetate (2.58 mL, 2.67 g, 23.6 mmol, 1.0 eq.) were dissolved in dry THF (100 mL). To this solution DBU (1,8-diazabicyclo[5.4.0] undec-7-ene) (3.53 mL, 3.59 g, 23.6 mmol, 1.0 eq.) was slowly added and the reaction mixture was refluxed over night. The solvent was removed by rotary evaporation and the crude product purified on a silica gel column (eluent: *n*-hexane/Et₂O = 3/1) to afford pale yellow crystals. Yield: 3.7 g, 81%. ¹H-NMR (δ , 20 °C, CDCl₃, 500 MHz): 8.76 (bs, 1H, NH), 6.64 (s, 1H, CHNH), 4.29 (q, 2H, OCH₂), 2.81 (t, 2H, cyclohexyl-CH₂), 2.54 (t, 2H, cyclohexyl-CH₂), 1.74 (m, 4H, cyclohexyl-CH₂), 1.34 (t, 3H, CH₃).

4,5,6,7-Tetrahydroisoindole.² A stirred mixture of 2H-isoindole-4,5,6,7-tetrahydro-1-carboxylic acid ethyl ester (1.05 g, 5.4 mmol, 1.0 eq.) and NaOH (1.2 g, 30 mmol, 5.5 eq.) was refluxed under N₂ in ethylene glycol (20 mL) for 60 min. The resulting solution was rapidly cooled on an ice bath and diluted with CH₂Cl₂ (100 mL). The mixture was thoroughly washed with water (2 x 100 mL; brine was added to reduce the emulsion), and the aqueous phase was extracted with CH₂Cl₂ (3 x 30 mL). The combined organic phases were washed with brine and dried over Na₂SO₄. The solvent was evaporated, and the resulting black solid was introduced into the following porphyrin synthesis immediately. Yield: 92%.

1,4-Dihydronaphthalene.³ To a solution of naphthalene (5.0 g, 39 mmol, 1.0 eq.) in dry Et₂O (80 mL) was added metallic Na (2.75 g, 120 mmol, 3.1 eq.) in small pieces over a period

of 10-15 minutes, and then a solution of HOBU^t (7.26 g, 98 mmol, 2.5 eq.) in dry Et₂O (10 mL) was slowly added over 10-20 min. After stirring at room temperature for 3 h, unreacted Na and solid NaOBU^t were removed by gravity filtration and washed with Et₂O (25 mL). The combined organic layer was washed with water (2 x 30 mL), dried over Na₂SO₄ and then the Et₂O was evaporated. According to ¹H NMR analysis, 1,4-dihydronaphthalene (1,4-DH) (3.45 g, Yield: 67.8 %) was obtained as the main product (75% 1,4-DH, 20% 1,2-DH, 5% naphthalene). ¹H-NMR (δ, 20 °C, CDCl₃, 500 MHz): 7.18-7.11 (m, 4H, ph^{1,2,3,4}), 5.93 (m, 2H, CH₂=CH₂), 3.40 (d, 4H, 2xCH₂) (integration revealed 75% 1,4-DH, 20% 1,2-DH, 5% naphthalene).

2-Chloro-1,2,3,4-tetrahydro-3-(phenylsulfonyl)-naphthalene.⁴ *N*-chlorosuccinimide (5.5 g, 42.2 mmol, 1.1 eq.) was suspended in dry CH₂Cl₂ (50 mL) under nitrogen and thiophenol (4.4 g, 40 mmol, 1.0 eq.) was added very slowly (exothermic reaction). The color changed to a dark orange solution while maintaining reflux conditions through the addition of the thiophenol. This solution was stirred at room temperature for 30 minutes. 1,4-Dihydronaphthalene (5.3 g, 41 mmol, 1.0 eq.) was diluted with dry CH₂Cl₂ (40 mL) and slowly added to the above reaction mixture at 0 °C, which was allowed to warm to room temperature and stirred for an additional 2 h after the addition. This mixture was placed into a freezer at -48 °C over night and the precipitated succinimide removed by filtration. The remaining solution was diluted with cold CH₂Cl₂ to about 50 ml total volume and cooled to 0 °C. Solid *m*-CPBA (3-chloroperbenzoic acid) (17.4 g, 101 mmol, 2.5 eq.) was added gradually and the mixture stirred for 1 h at room temperature. An ice cold 10% aq. Na₂SO₃ solution was added and the mixture transferred into a separator funnel. The organic phase was separated, washed with a 10% aq. Na₂SO₃ solution and a 10% aq. Na₂CO₃ solution, dried over Na₂SO₄ and the solvent evaporated to dryness. The resulting white needles were recrystallized from EtOH and washed with *n*-hexane to yield 55% of the product. TLC,

CH₂Cl₂, *R_f* = 0.8 on silica. ¹H-NMR (δ, 20 °C, CDCl₃, 500 MHz): 7.95-7.92 (m, 2H, S-phenyl-CH), 7.72-7.67 (m, 1H, S-phenyl-CH), 7.62-7.57 (m, 2H, S-phenyl-CH), 7.21-7.18 (m, 2H, phenyl-CH), 7.14-7.09 (m, 2H, phenyl-CH), 4.87-4.82 (q, 1H, ³*J*_{HH} = 4.5 Hz, CHCl), 3.75-3.69 (m, 1H, CHS), 3.51-3.44 (dd, 1H, ³*J*_{HH} = 16.6 Hz, ⁴*J*_{HH} = 4.7 Hz, CH₂), 3.35-3.27 (dd, 1H, ³*J*_{HH} = 16.9 Hz, ⁴*J*_{HH} = 6.8 Hz, CH₂), 3.20-3.06 (m, 2H, CH₂).

4,9-Dihydro-2H-benz[f]isoindole-1-carboxylic acid ethyl ester.² Ethyl isocyanoacetate (2.7 mL, 2.8 g, 24.7 mmol, 1.2 eq.) was dissolved in 100 mL of dry THF. *t*-BuOK (62 mL, 1 M in THF, 3.0 eq.) was slowly added to this solution. A solution of α-chlorosulfone (6.3 g, 20.5 mmol, 1.0 eq.) in 25 mL of THF was quickly added to the mixture, which was stirred under N₂ for 10 min at rt and then refluxed under N₂ for 40 min. The mixture was cooled to rt, and its volume was reduced to about 15 mL by rotary evaporation. CH₂Cl₂ (100 mL) was added to the mixture, and the resulting solution was washed with water (100 mL) and then with brine (50 mL) and dried over Na₂SO₄. After evaporation of the solvent, the residue was recrystallized from ethanol to give the ester as yellow crystals. Yield 2.3 g (46%). TLC, CH₂Cl₂, *R_f* = 0.8 on silica, dark spot in the UV light. ¹H-NMR (δ, 20 °C, CDCl₃, 500 MHz): 8.95 (bs, 1H, NH), 7.33-7.30 (m, 2H, phenyl-CH), 7.21-7.17 (m, 2H, phenyl-CH), 6.82 (d, 1H, ³*J*_{HH} = 2.8 Hz, CHNH), 4.40-4.33 (q, 2H, ³*J*_{HH} = 7.2 Hz, OCH₂), 4.18 (s, 2H, CH₂), 3.90 (s, 2H, CH₂), 1.40 (t, 3H, ³*J*_{HH} = 7.1 Hz, CH₃).

4,9-Dihydro-2H-benz[f]isoindole.² A stirred mixture of 4,9-dihydro-2H-benz[f]isoindole-1-carboxylic acid ethyl ester (1.09 g, 4.5 mmol, 1.0 eq.) and NaOH (0.96 g, 30 mmol, 5.3 eq.) was refluxed under N₂ in ethylene glycol (20 mL) for 30 min. The resulting solution was rapidly cooled on an ice bath and diluted with CH₂Cl₂ (100 mL). The mixture was thoroughly washed with water (2 x 100 mL; brine was added to reduce the emulsion), and the aqueous phase was extracted with CH₂Cl₂ (3 x 30 mL). The combined organic phases were washed

with brine and dried over Na_2SO_4 . The solvent was evaporated, and the resulting black solid was introduced into the following porphyrin synthesis immediately. Yield: 90%.

NMR-Spectra

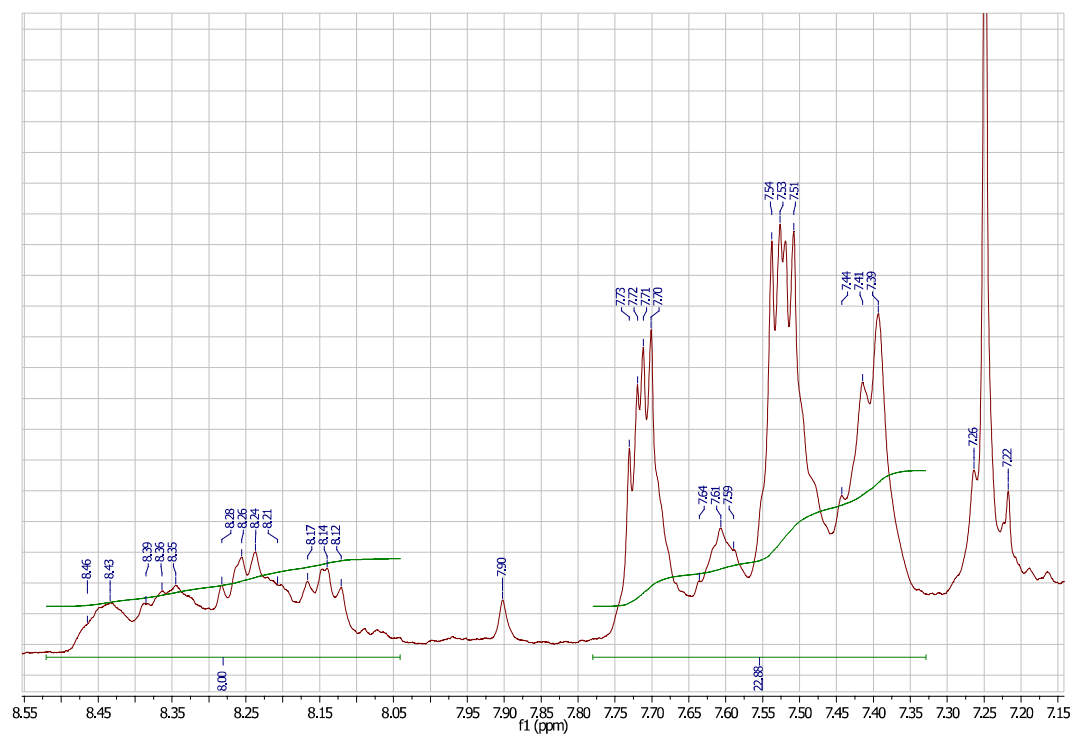


Figure S1. ^1H NMR-spectrum of **1NF** in CDCl_3 (only the aromatic region is shown).

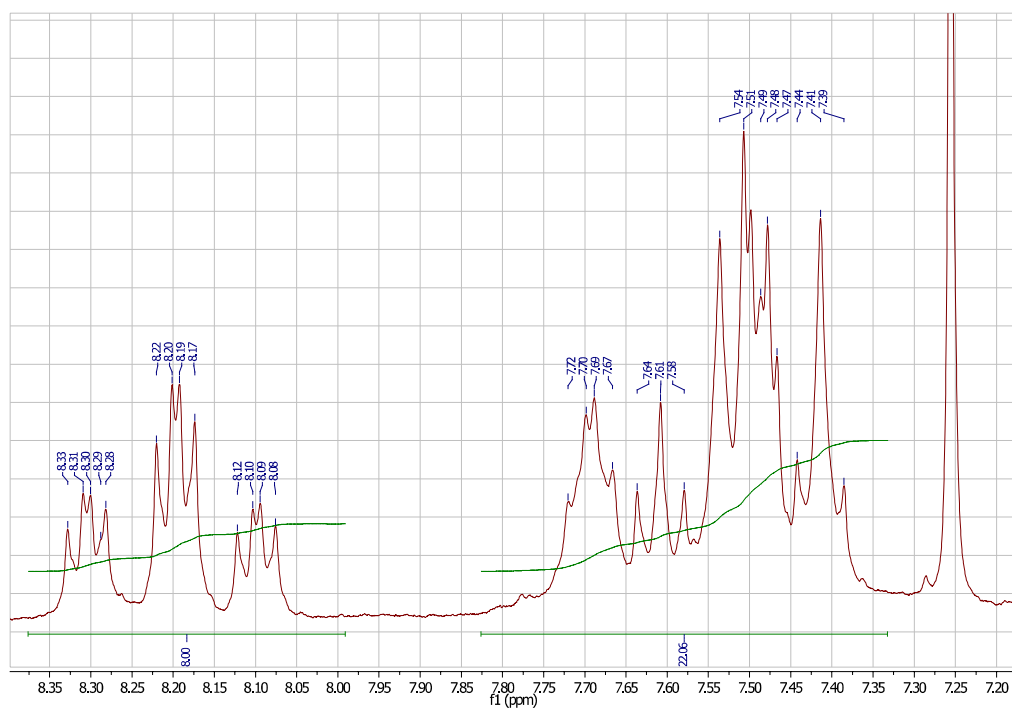


Figure S2. $^1\text{H-NMR}$ spectrum of **2NF** in CDCl_3 (only the aromatic region is shown).

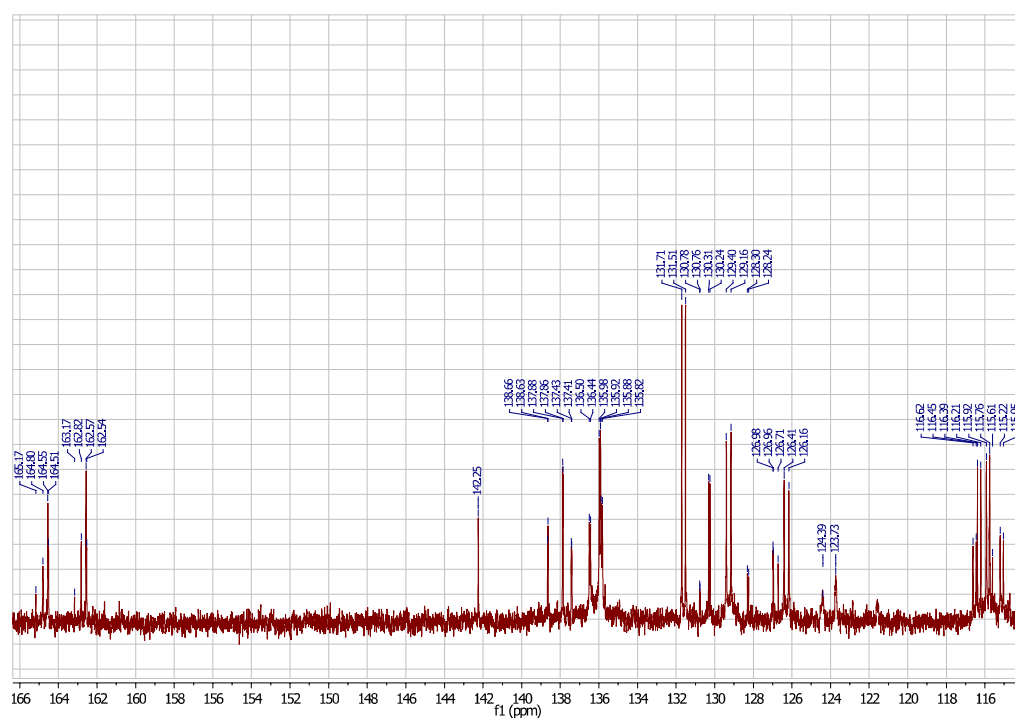


Figure S3. $^{13}\text{C-NMR}$ spectrum of **2NF** in CDCl_3 (only the aromatic region is shown).

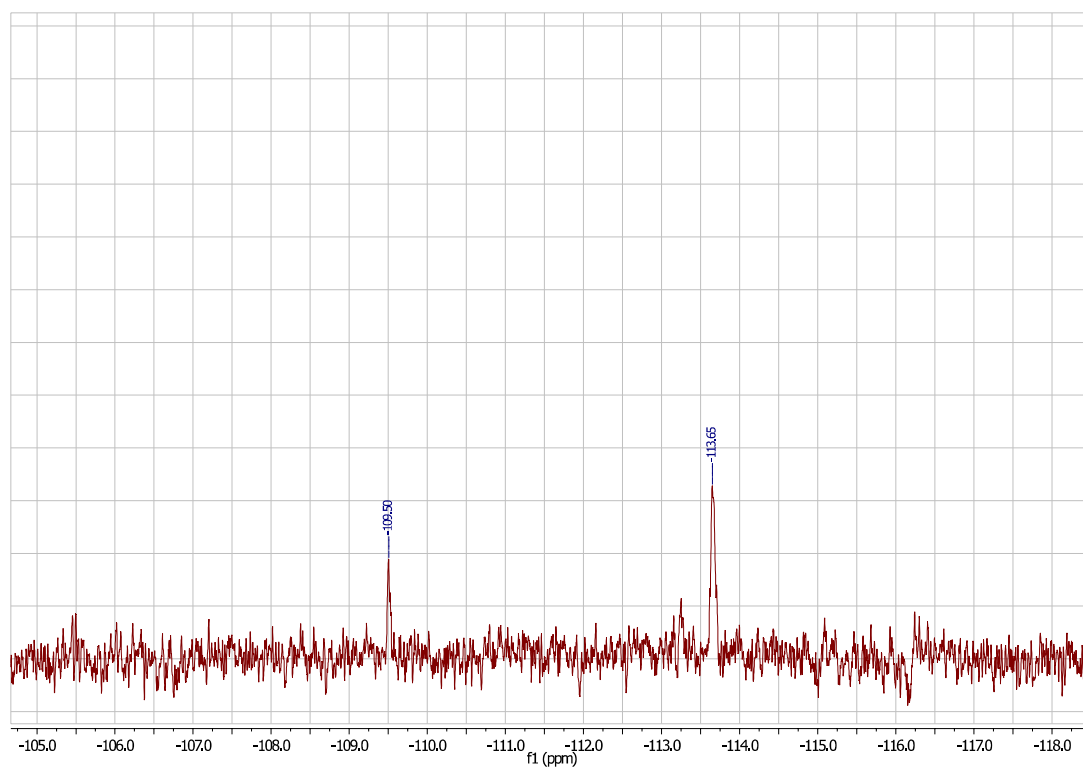


Figure S4. ^{19}F -NMR spectrum of 2NF in CDCl_3 .

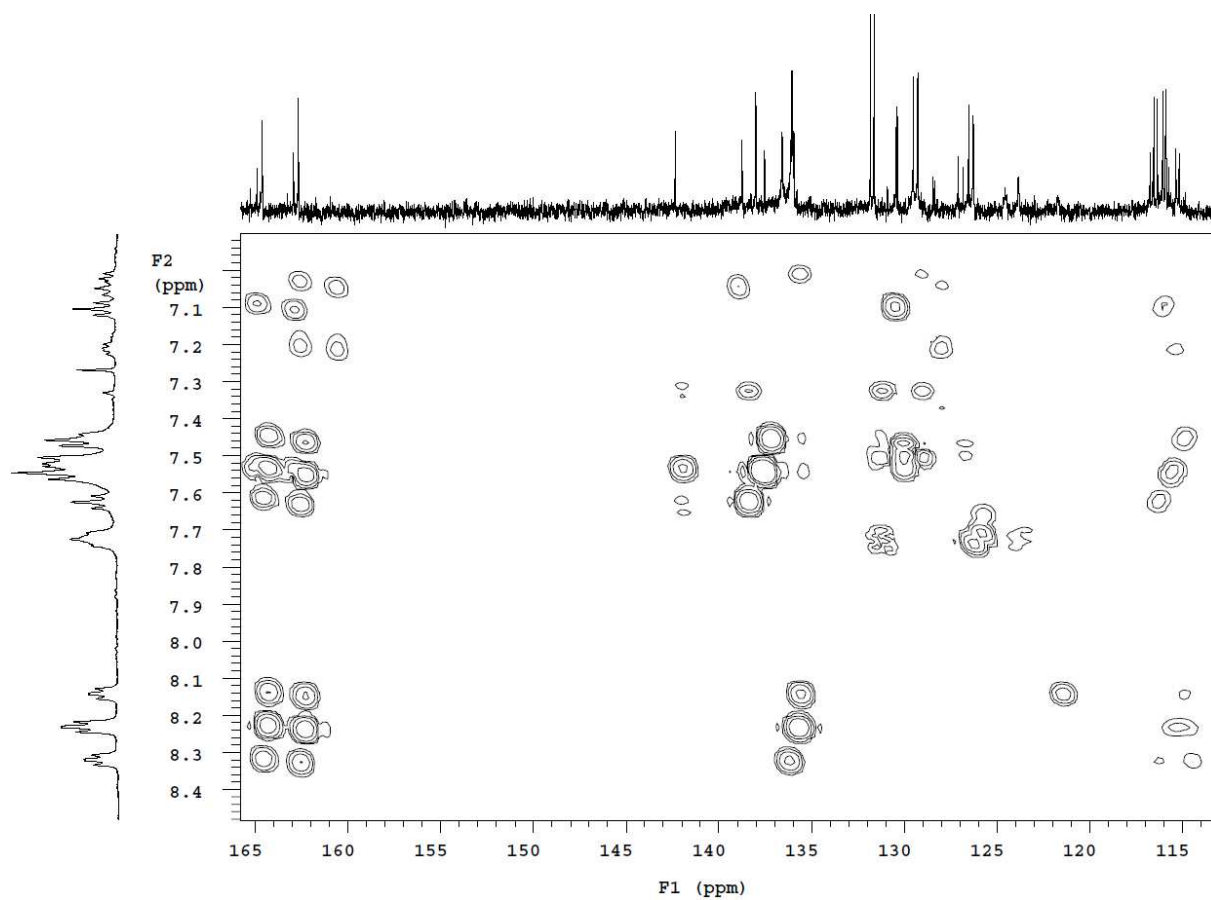


Figure S5. 2D ^1H - ^{13}C NMR-HMBC spectrum of 2NF in CDCl_3 .

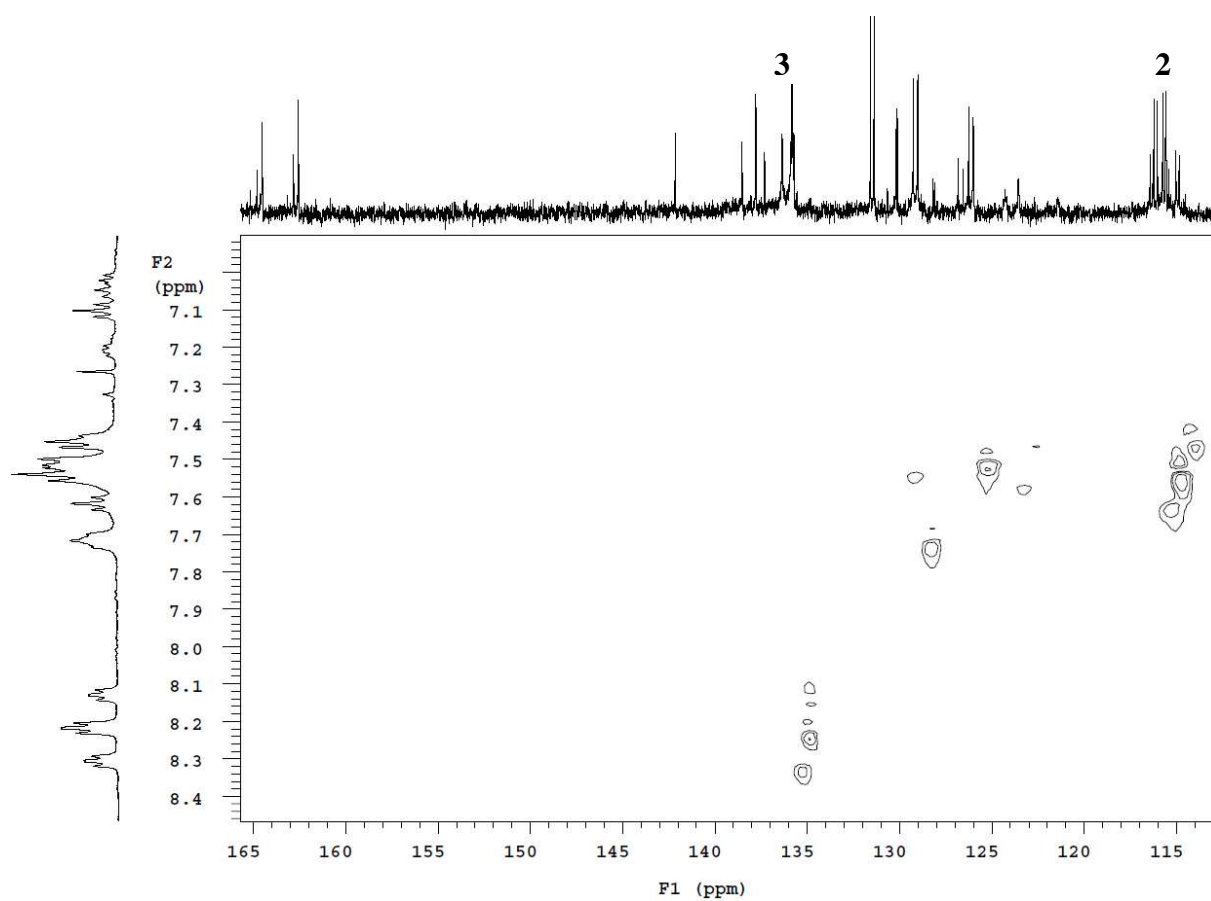
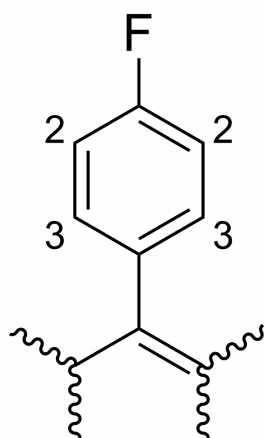


Figure S6. 2D ^1H - ^{13}C NMR-HSQC spectrum of **2NF** in CDCl_3 .

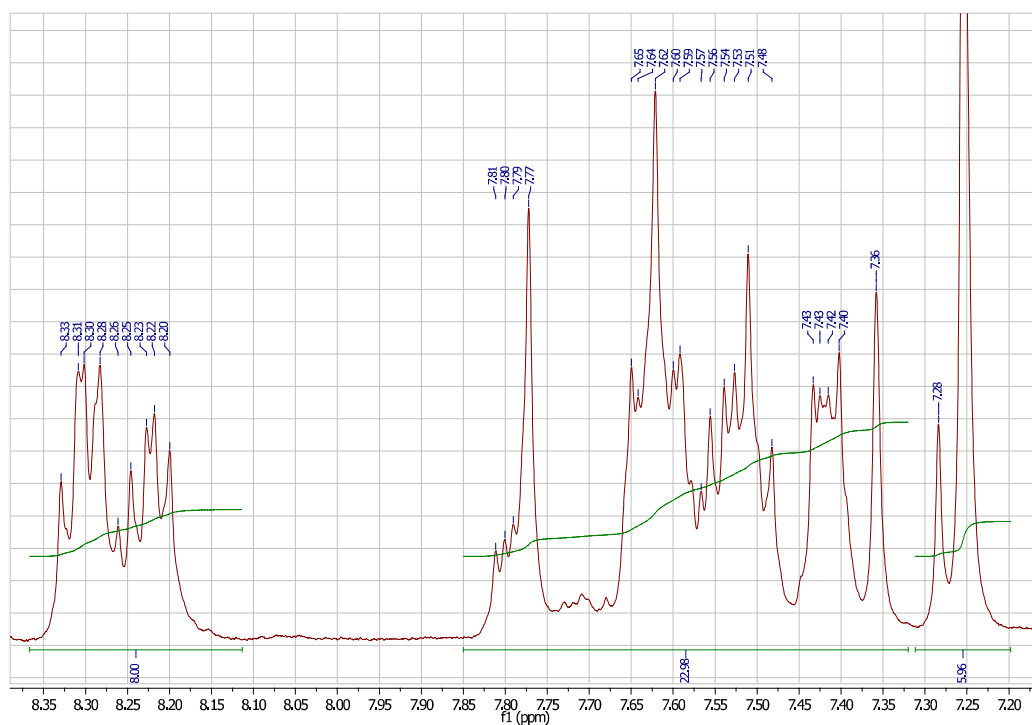


Figure S7. $^1\text{H-NMR}$ spectrum of **3NF** in CDCl_3 (only the aromatic region is shown).

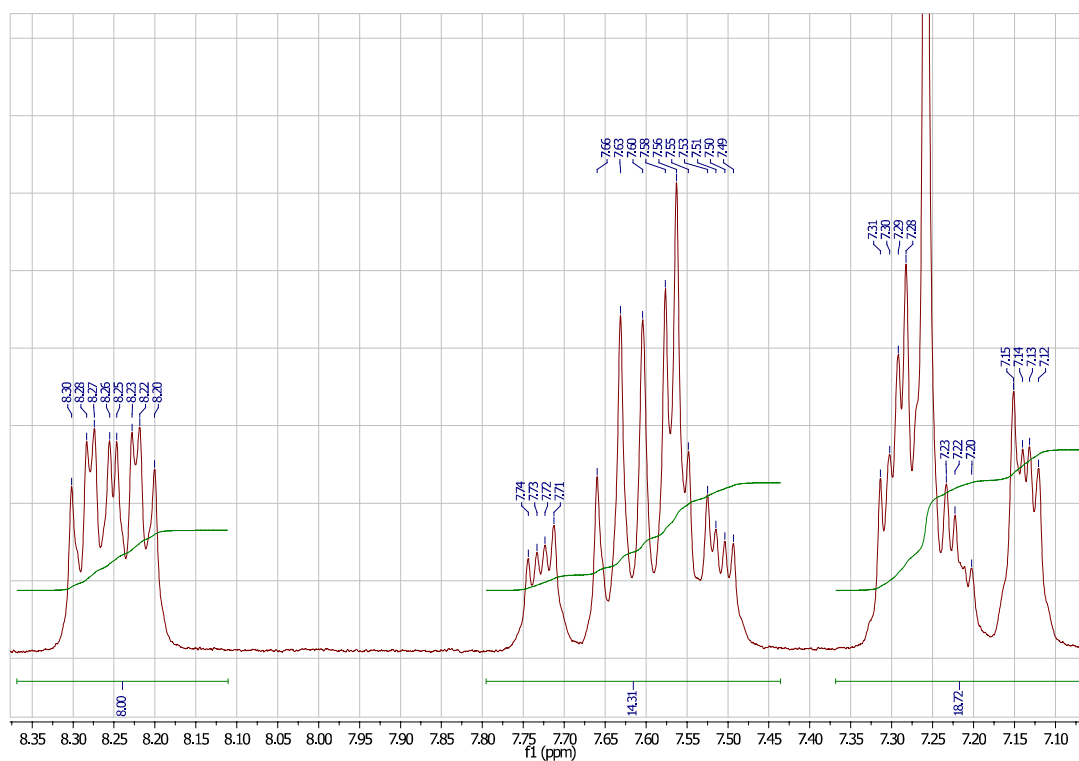


Figure S8. $^1\text{H-NMR}$ spectrum of **Pd1NF** in CDCl_3 (only the aromatic region is shown).

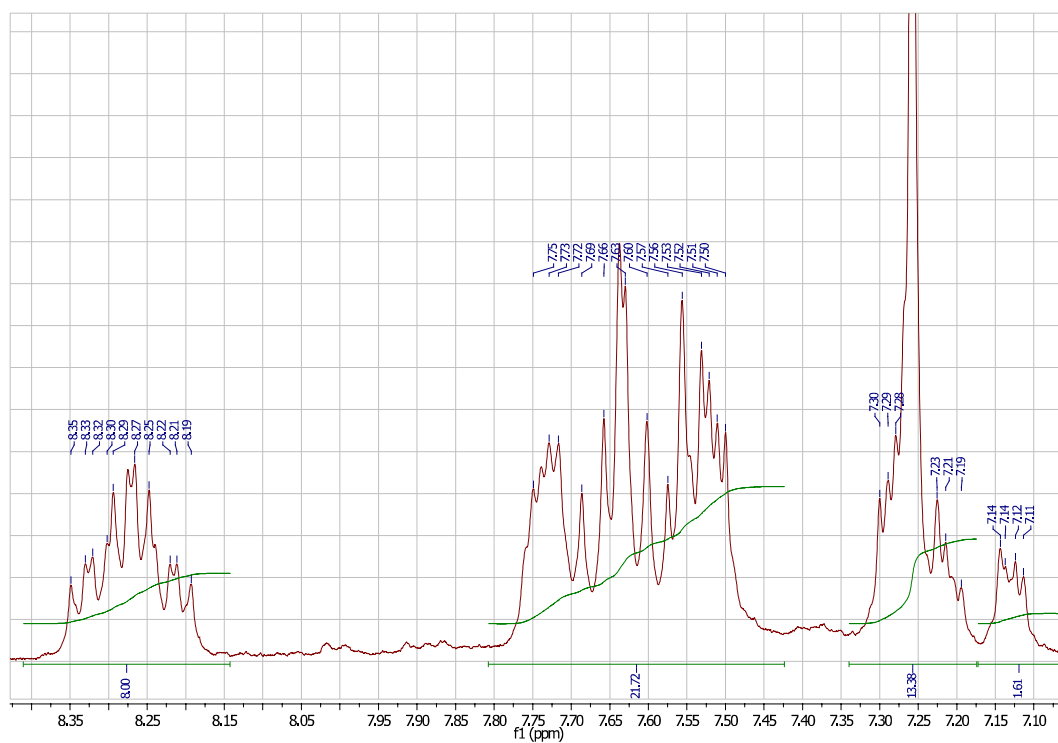


Figure S9. $^1\text{H-NMR}$ spectrum of **Pd2NF** in CDCl_3 (only the aromatic region is shown).

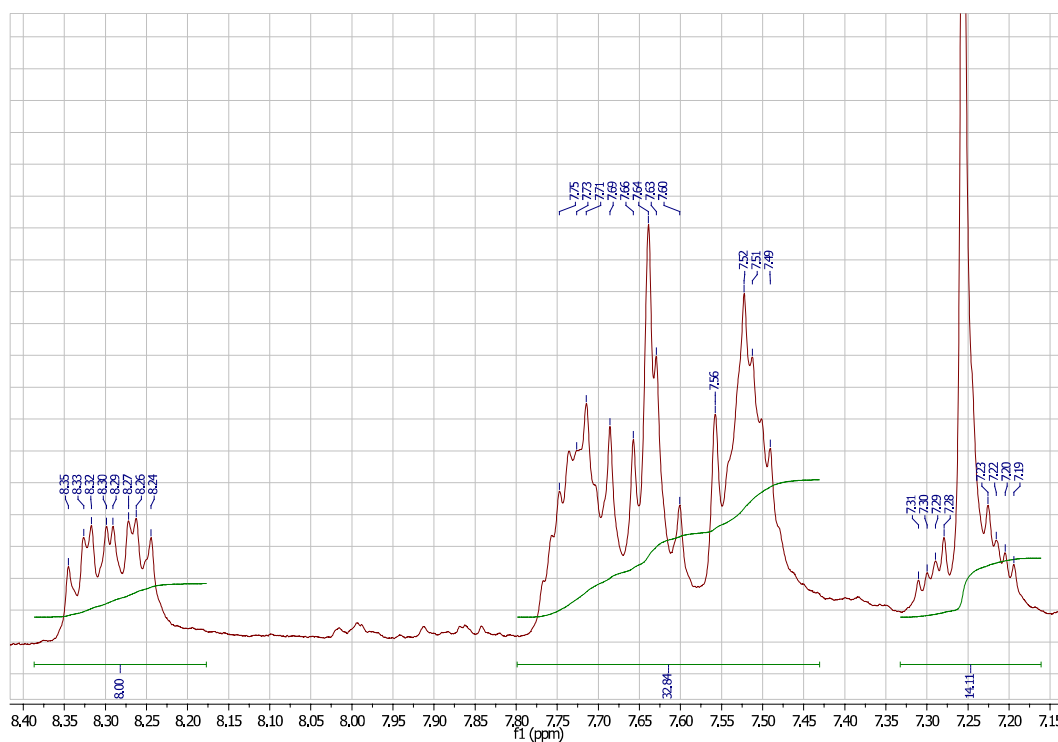


Figure S10. $^1\text{H-NMR}$ spectrum of **Pd3NF** in CDCl_3 (only the aromatic region is shown).

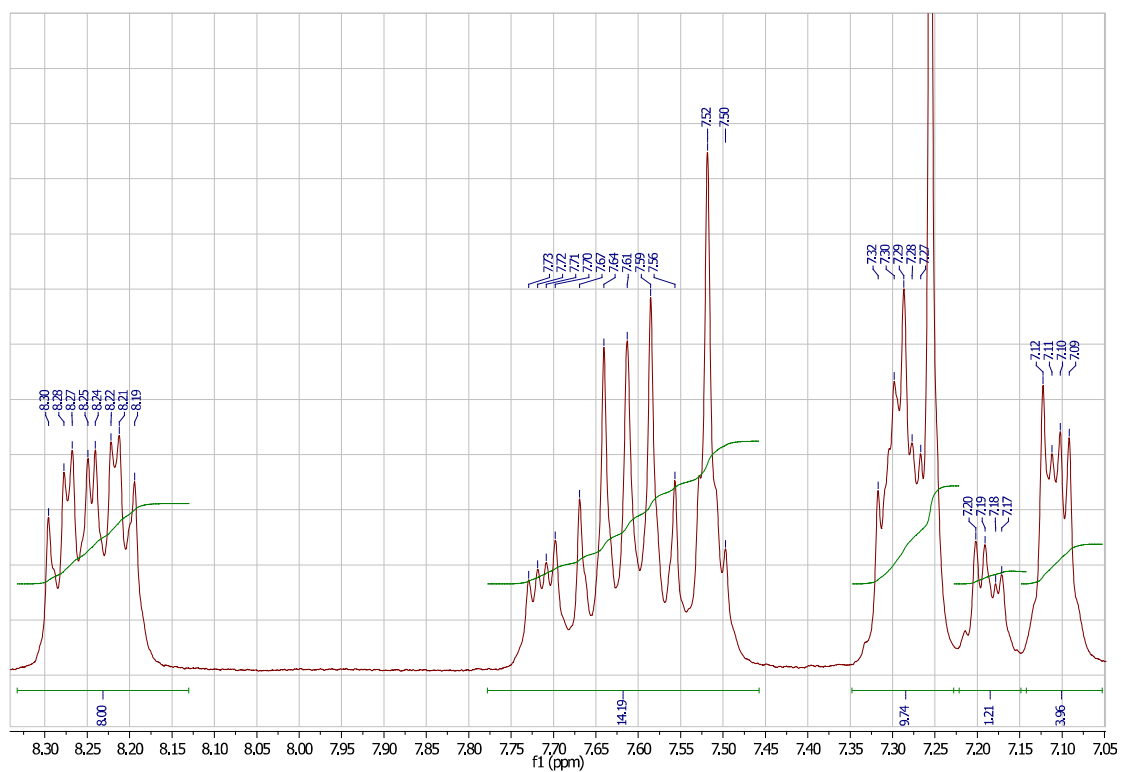


Figure S11. $^1\text{H-NMR}$ spectrum of **Pt1NF** in CDCl_3 (only the aromatic region is shown).

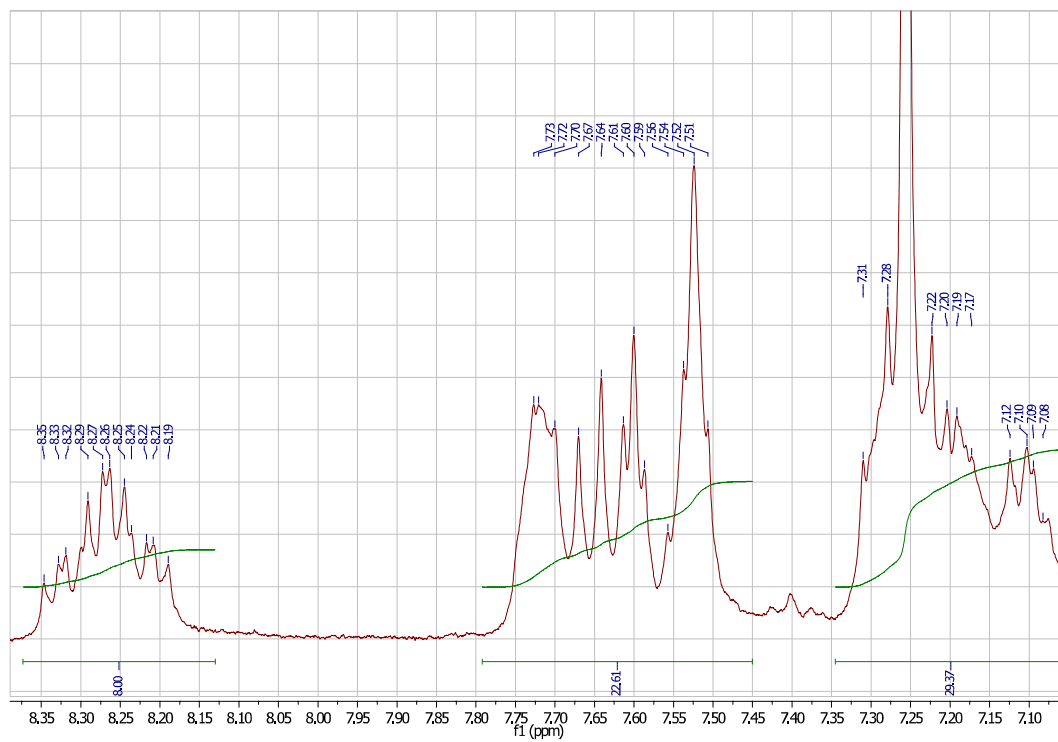


Figure S12. $^1\text{H-NMR}$ spectrum of **Pt2NF** in CDCl_3 (only the aromatic region is shown).

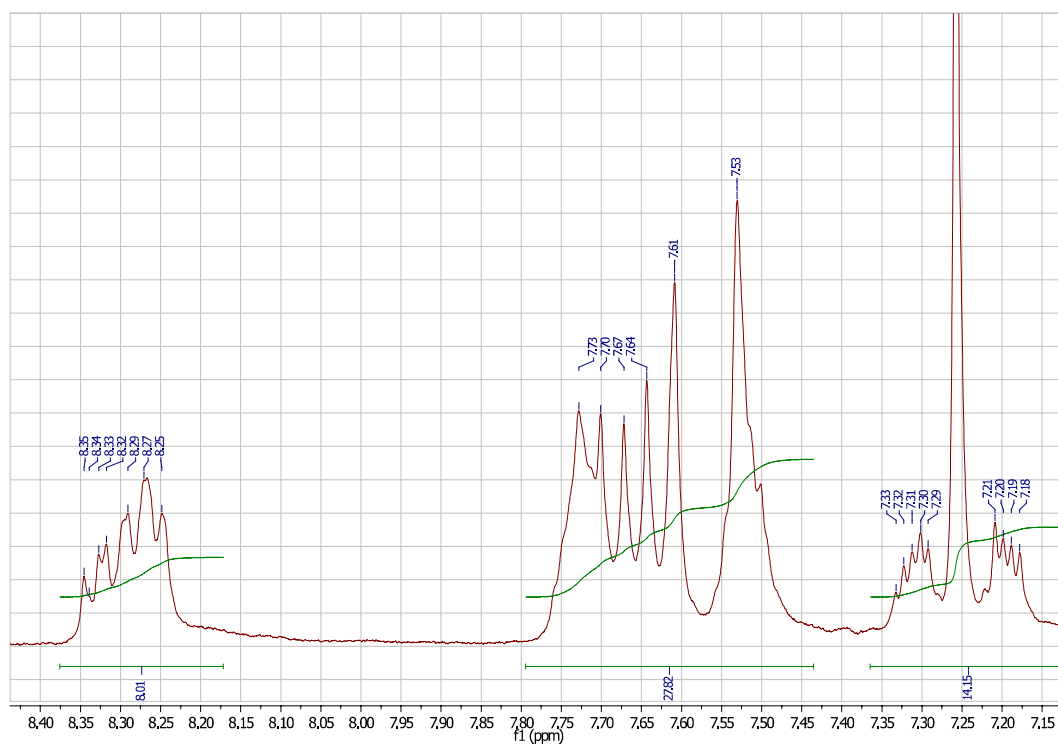


Figure S13. $^1\text{H-NMR}$ spectrum of **Pt3NF** in CDCl_3 (only the aromatic region is shown).

Photo Physical Data

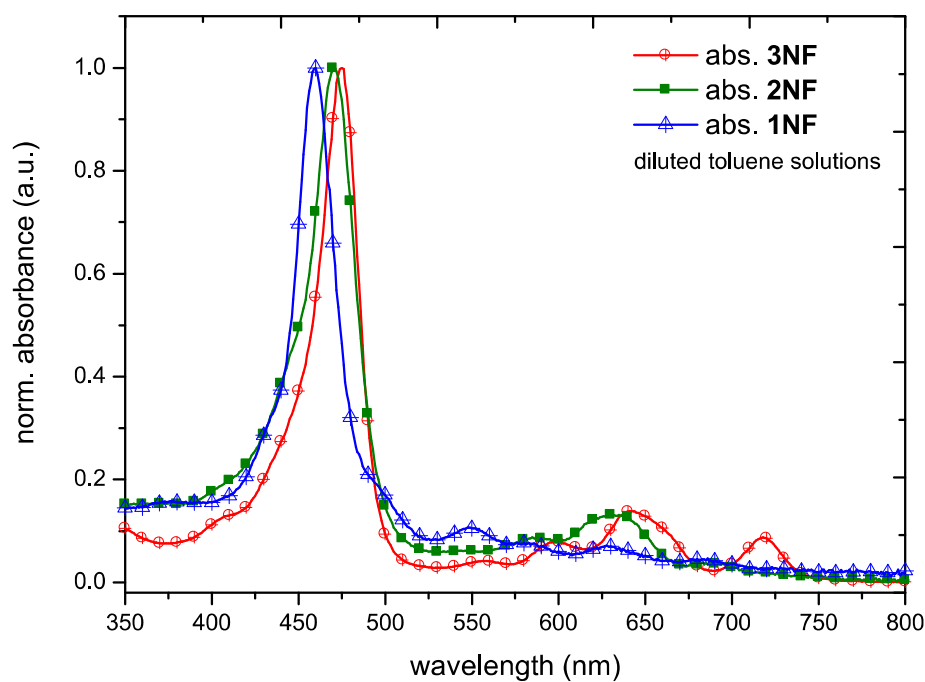


Figure S14. Absorption spectra of the three main ligand fractions **1NF**, **2NF** and **3NF** after Lindsey condensation measured in diluted toluene solution at room temperature.

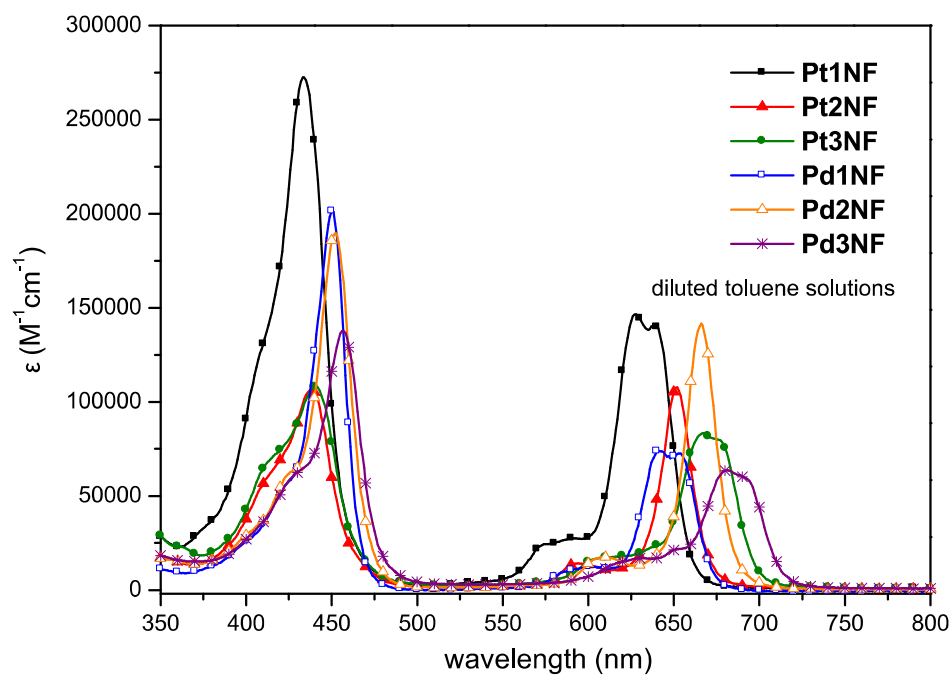


Figure S15. Absorption spectra of all complexes in diluted toluene solution at room temperature.

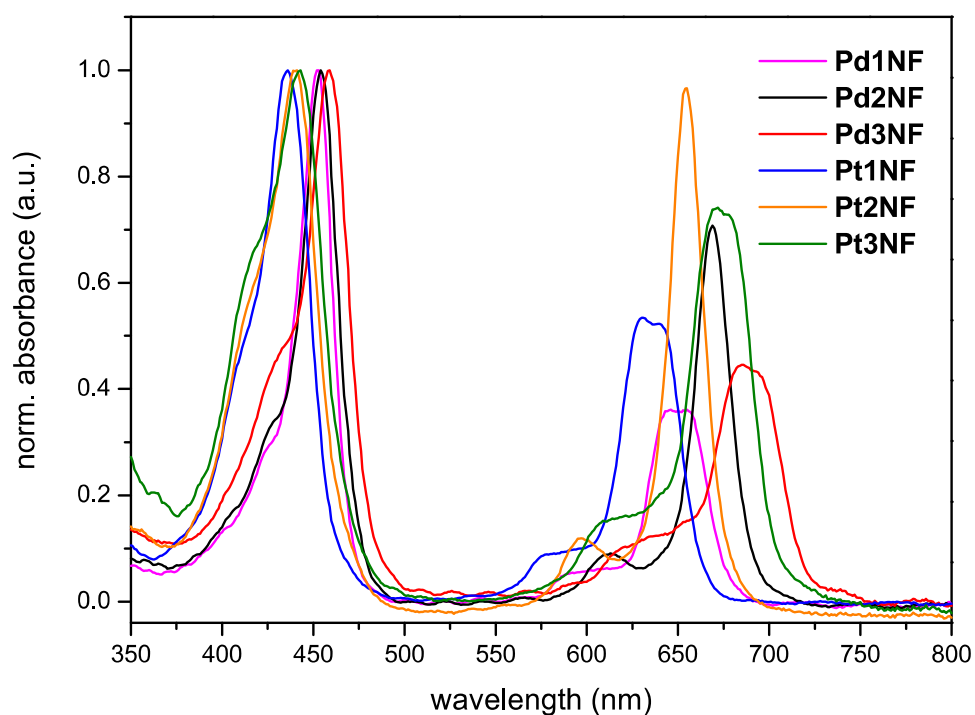


Figure S16. Normalised absorption spectra of polymeric sensor films (polystyrene film, 1% of the indicator, w/w; 2.5 μm thick film).

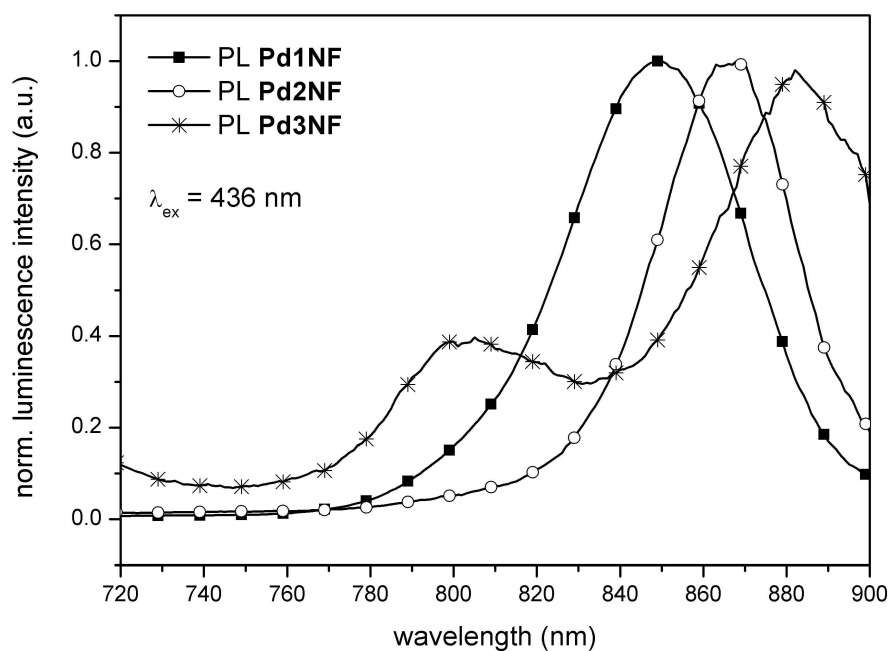


Figure S17. Emission spectra of palladium complexes measured in toluene ($\lambda_{\text{exc}} = 436$ nm).

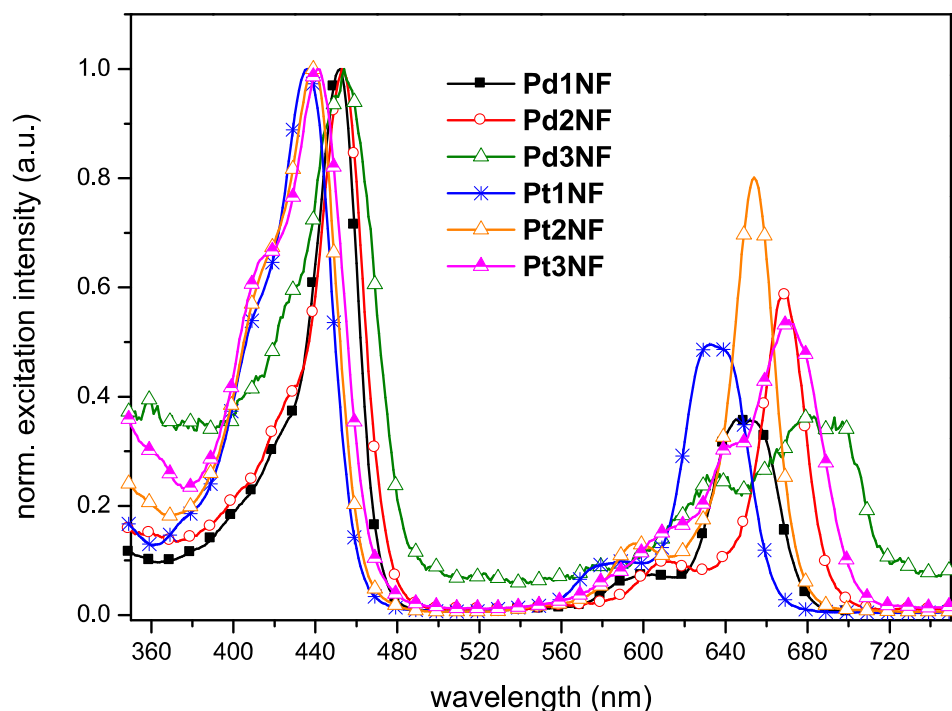


Figure S18. Excitation spectra of **Pd1NF** ($\lambda_{\text{em}} = 840$ nm), **Pd2NF** ($\lambda_{\text{em}} = 852$ nm), **Pd3NF** ($\lambda_{\text{em}} = 850$ nm), **Pt1NF** ($\lambda_{\text{em}} = 815$ nm), **Pt2NF** ($\lambda_{\text{em}} = 832$ nm) and **Pt3NF** ($\lambda_{\text{em}} = 850$ nm) measured in toluene (absorbances at the excitation wavelength of 436 nm were 0.1 for all complexes).

Oxygen quenching

Film

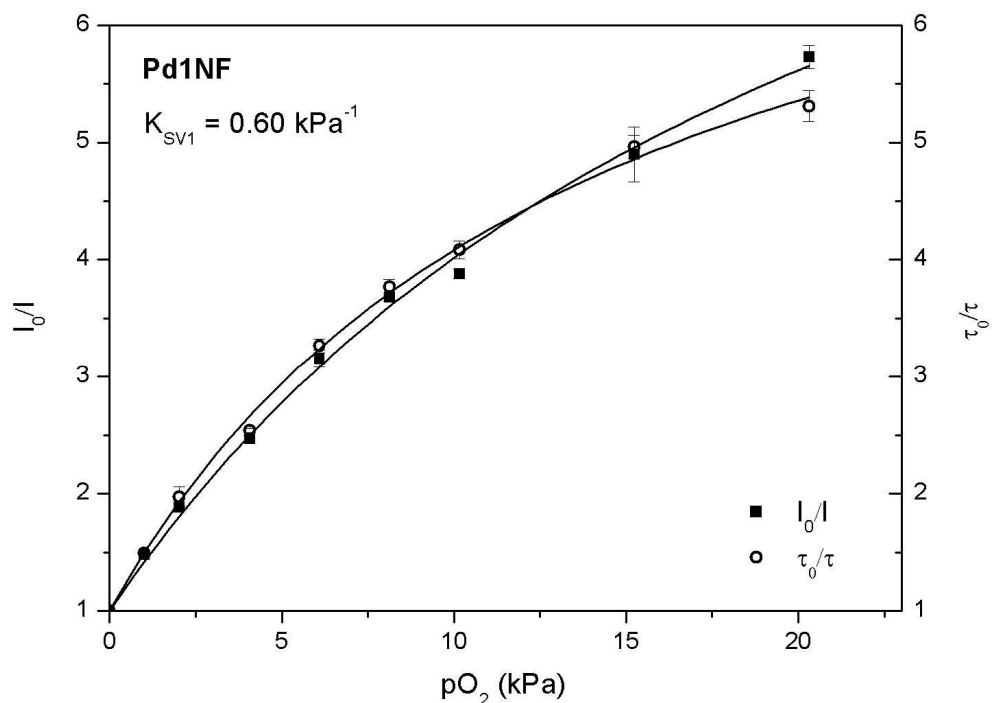


Figure S19. Stern-Volmer plots for **Pd1NF** embedded in polystyrene (at 25 °C). Curve fitting is performed using a “two-site” model.⁵

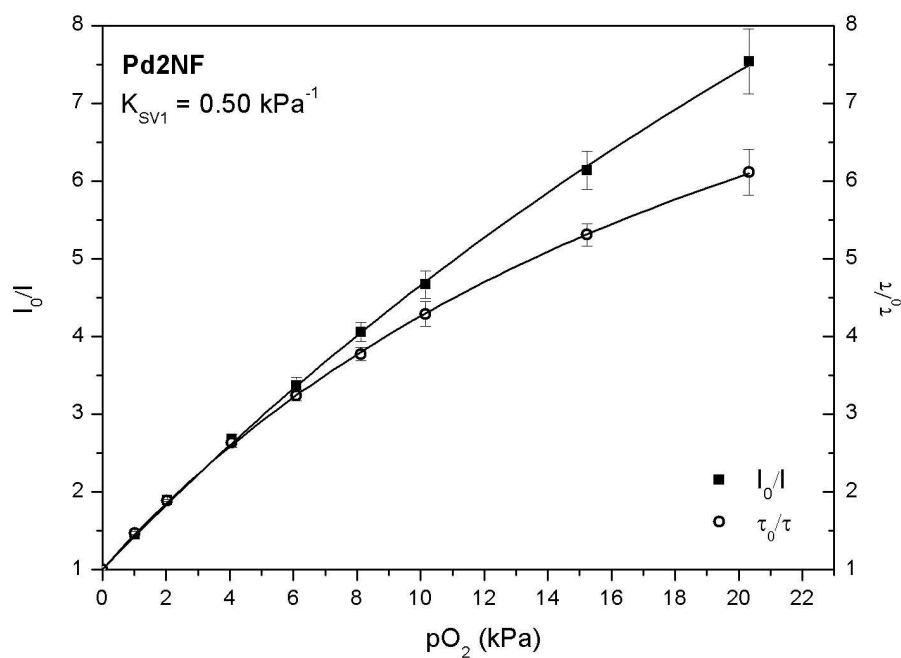


Figure S20. Stern-Volmer plots for **Pd2NF** embedded in polystyrene (at 25 °C). Curve fitting is performed using a “two-site” model.⁵

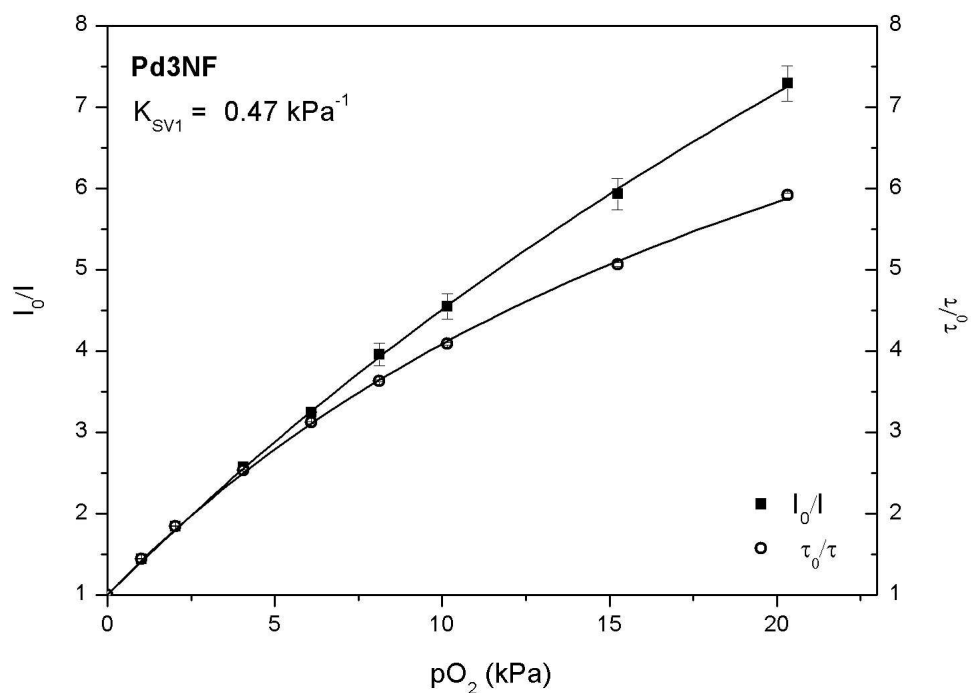


Figure S21. Stern-Volmer plots for **Pd3NF** embedded in polystyrene (at 25 °C). Curve fitting is performed using a “two-site” model.⁵

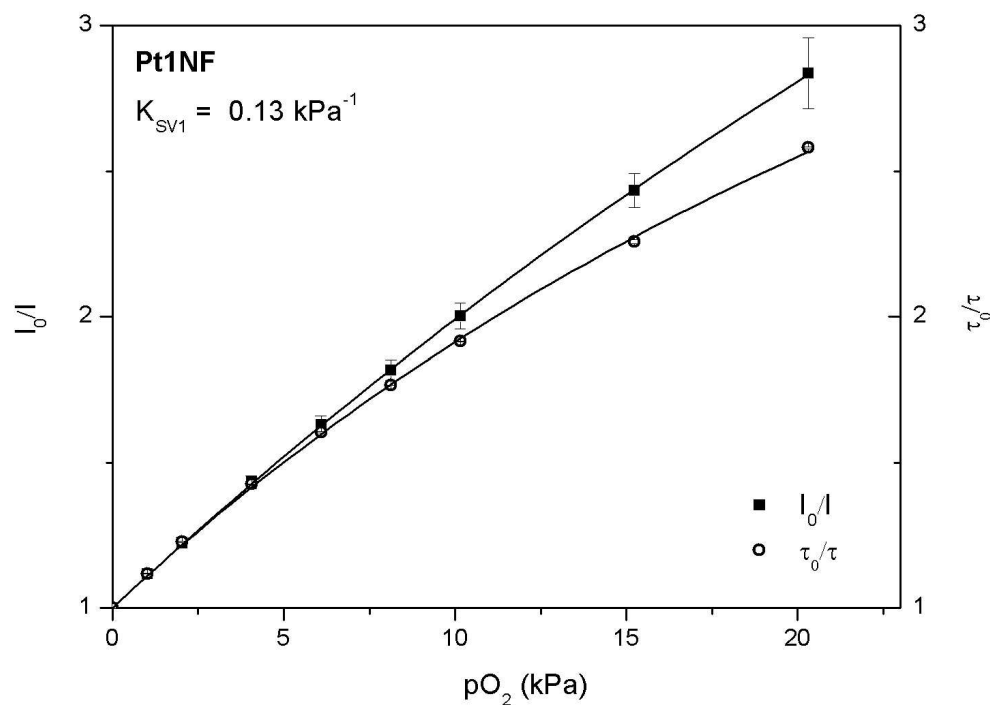


Figure S22. Stern-Volmer plots for **Pt1NF** embedded in polystyrene (at 25 °C). Curve fitting is performed using a “two-site” model.⁵

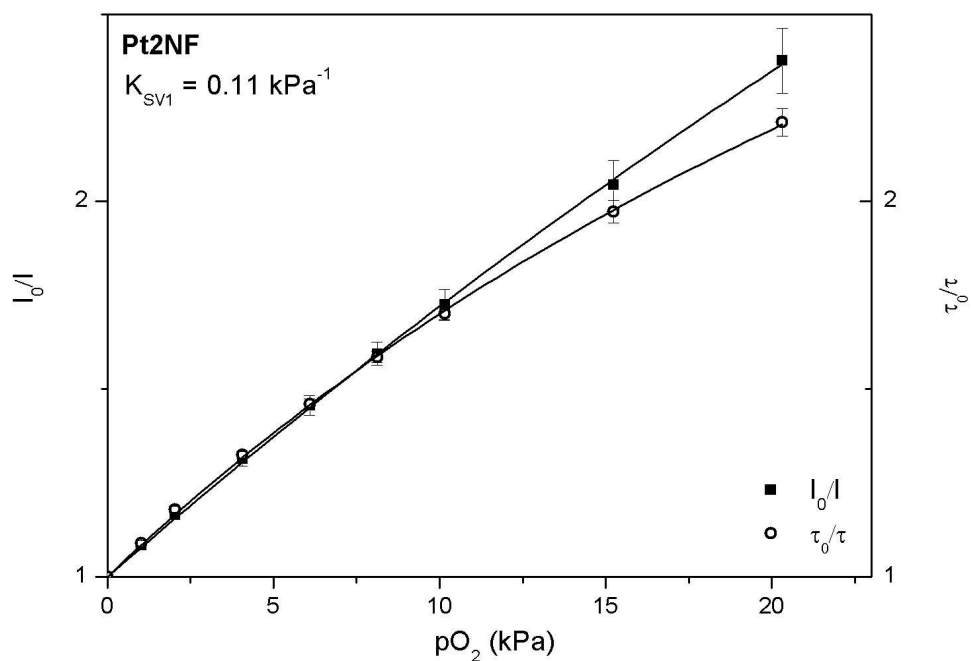


Figure S23. Stern-Volmer plots for **Pt2NF** embedded in polystyrene (at 25 °C). Curve fitting is performed using a “two-site” model.⁵

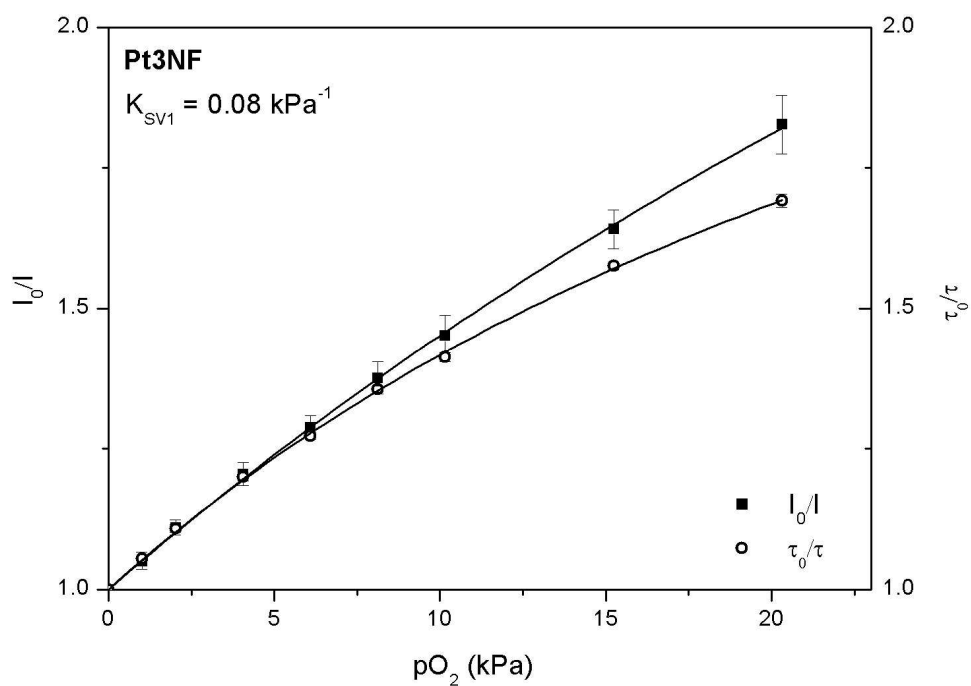


Figure S24. Stern-Volmer plots for **Pt3NF** embedded in polystyrene (at 25 °C). Curve fitting is performed using a “two-site” model.⁵

Solution

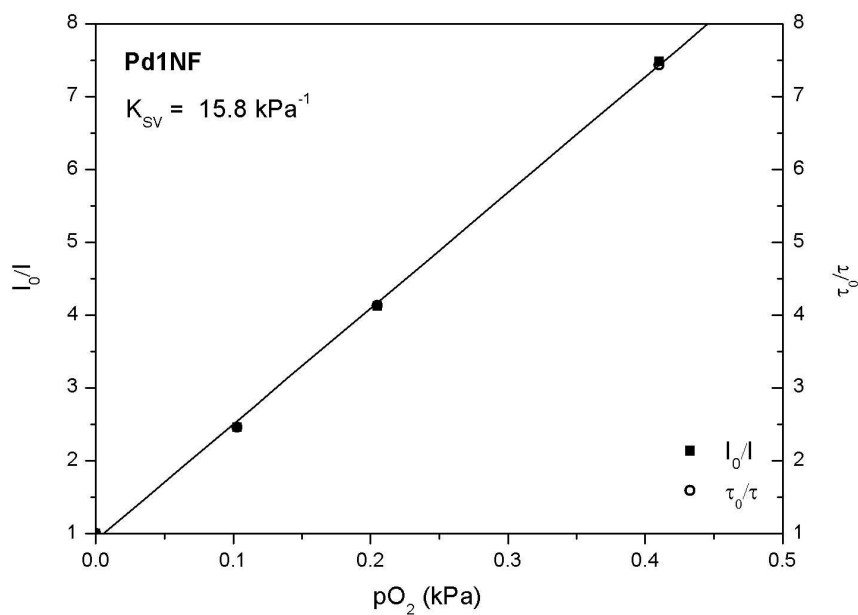


Figure S25. Stern-Volmer plots for **Pd1NF** in toluene (at 25 °C).

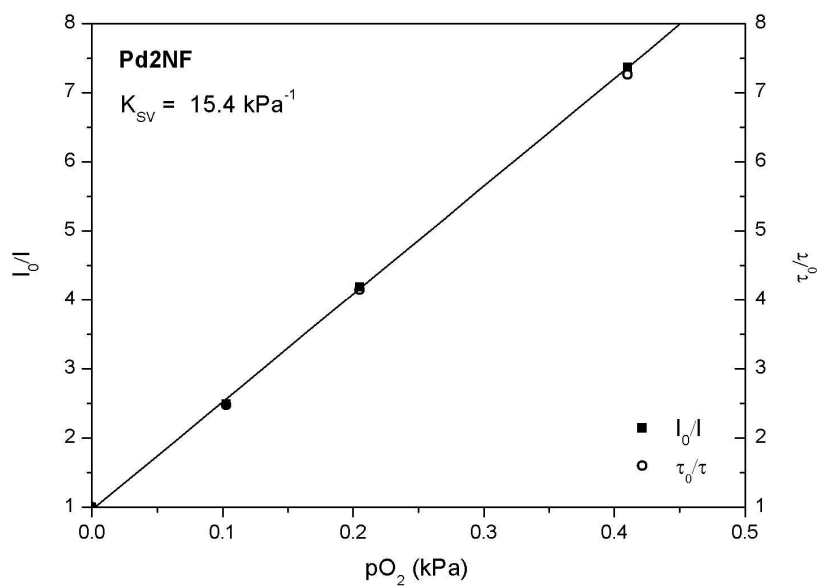


Figure S26. Stern-Volmer plots for **Pd2NF** in toluene (at 25 °C).

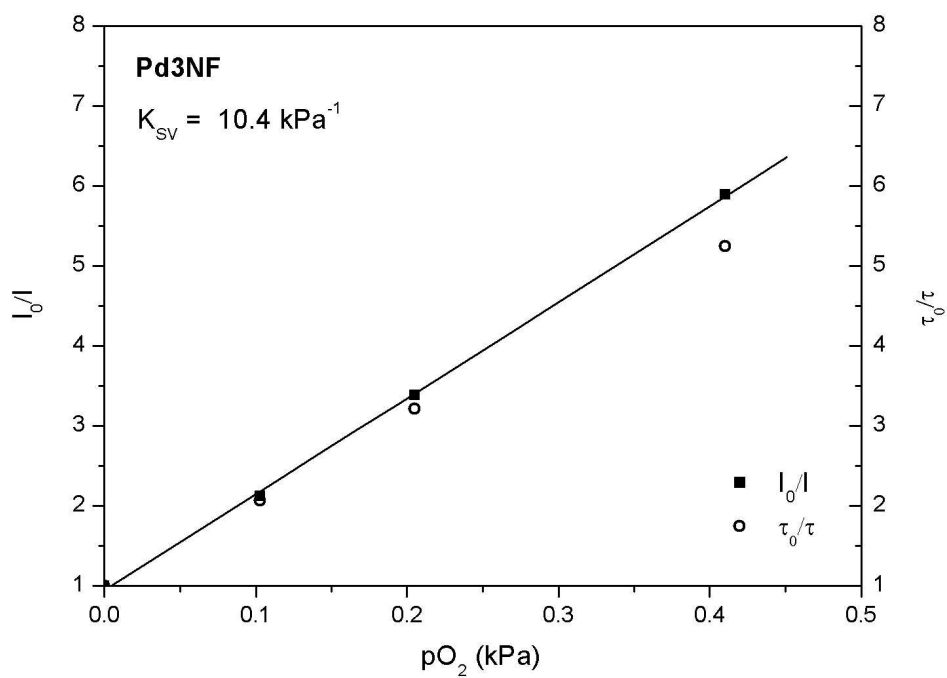


Figure S27. Stern-Volmer plots for **Pd3NF** in toluene (at 25 °C).

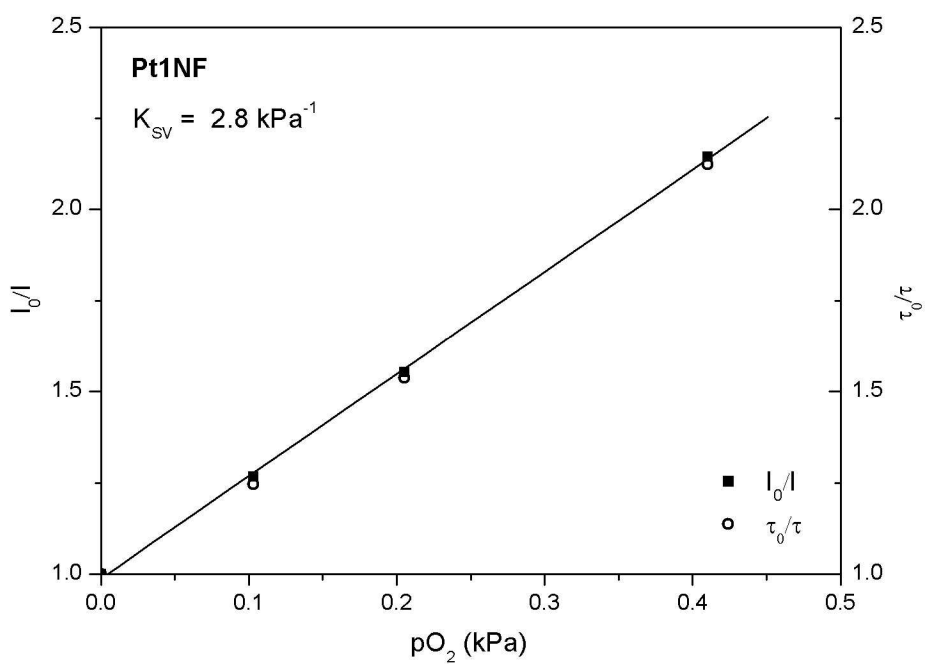


Figure S28. Stern-Volmer plots for **Pt1NF** in toluene (at 25 °C).

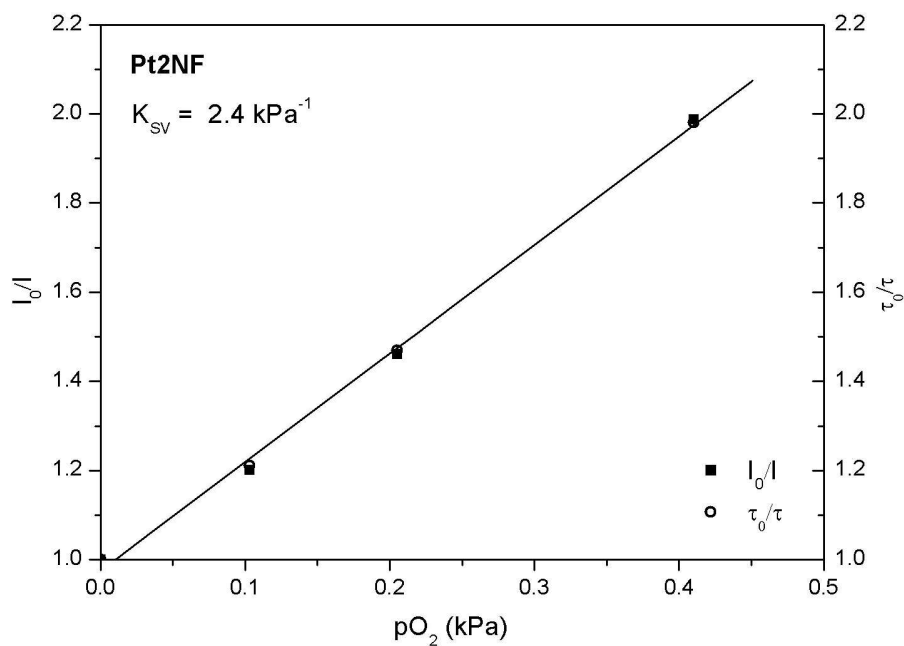


Figure S29. Stern-Volmer plots for **Pt2NF** in toluene (at 25 °C).

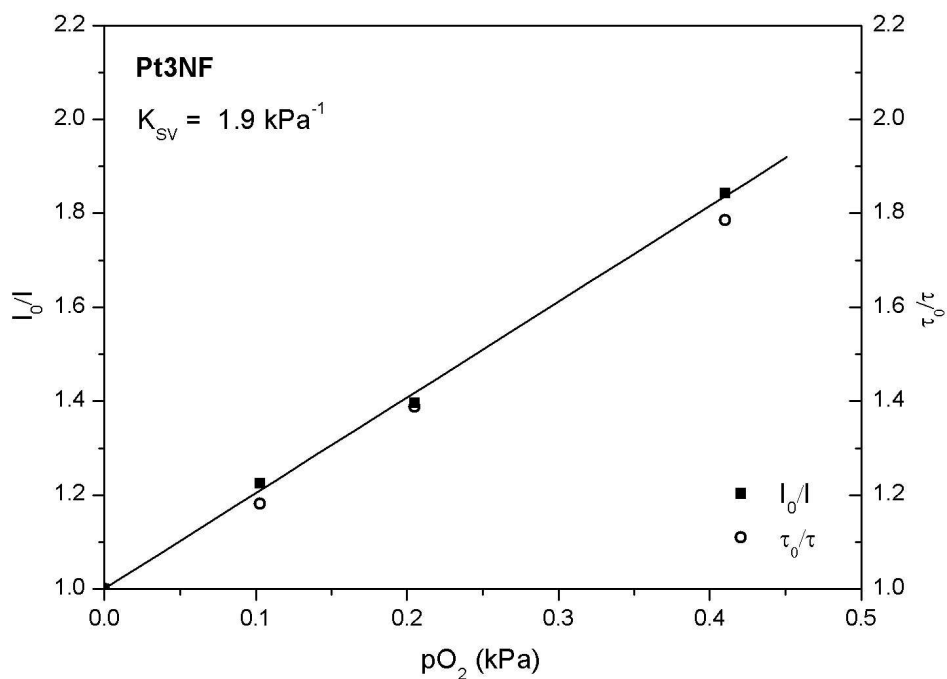


Figure S30. Stern-Volmer plots for **Pt3NF** in toluene (at 25 °C).

Photostability measurements

Film

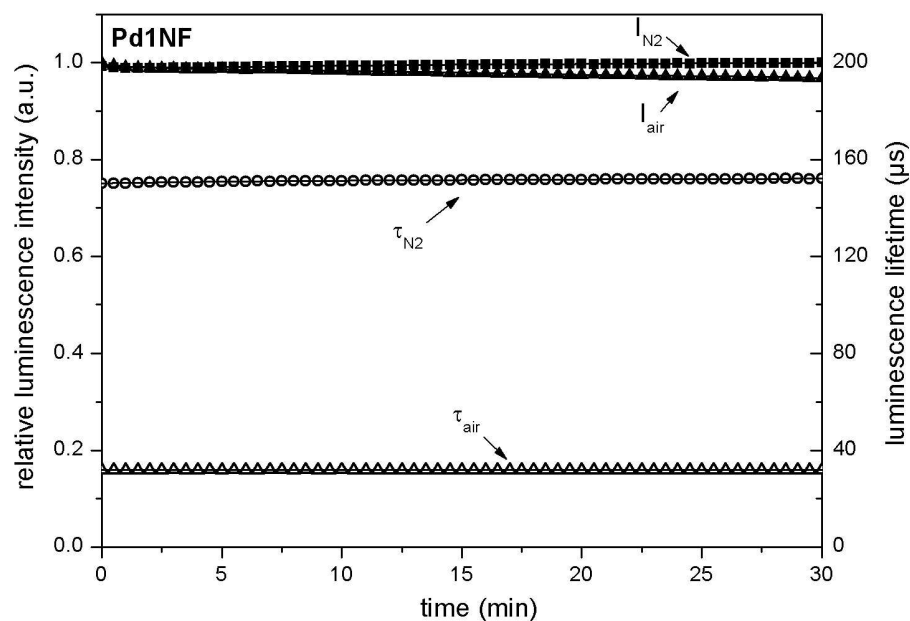


Figure S31. Photo-degradation curves for the metalloporphyrin **Pd1NF** embedded in a polystyrene film (1% of the indicator, w/w; 2.5 μm thick film). Irradiation is performed with a blue LED ($\lambda_{\text{max}} = 450 \text{ nm}$, flux: $200 \mu\text{mols}^{-1}\text{m}^{-2}\mu\text{A}$).

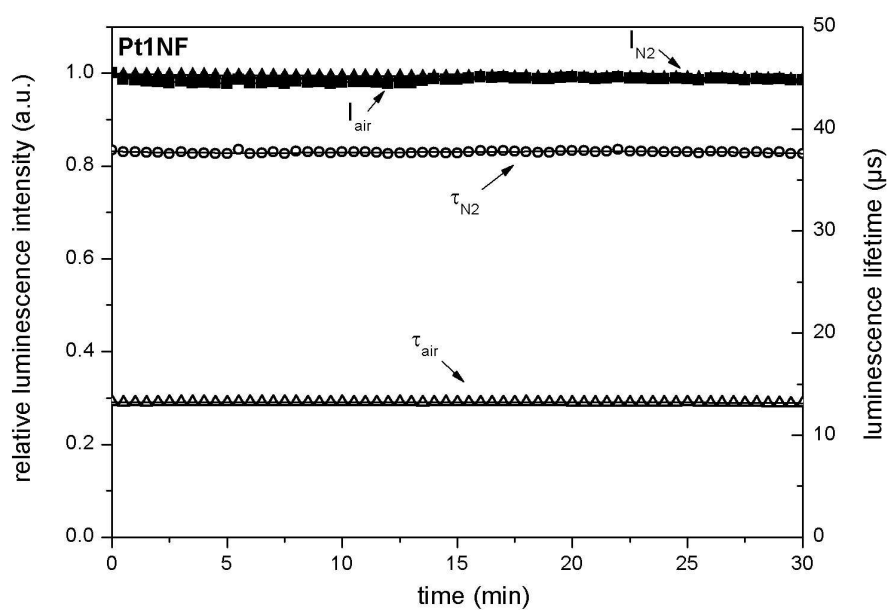


Figure S32. Photo-degradation curves for the metalloporphyrin **Pt1NF** embedded in a polystyrene film (1% of the indicator, w/w; 2.5 μm thick film). Irradiation is performed with a blue LED ($\lambda_{\text{max}} = 450 \text{ nm}$, flux: $200 \mu\text{mols}^{-1}\text{m}^{-2}\mu\text{A}$).

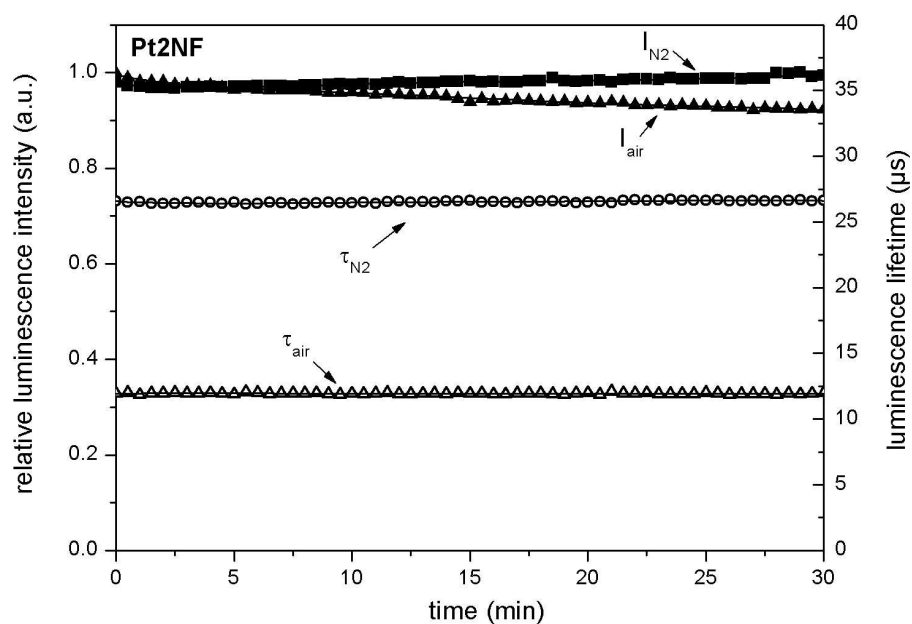


Figure S33. Photo-degradation curves for the metalloporphyrin **Pt2NF** embedded in a polystyrene film (1% of the indicator, w/w; 2.5 μm thick film). Irradiation is performed with a blue LED ($\lambda_{max} = 450$ nm, flux: $200 \mu\text{mols}^{-1}\text{m}^{-2}\mu\text{A}$).

Solution

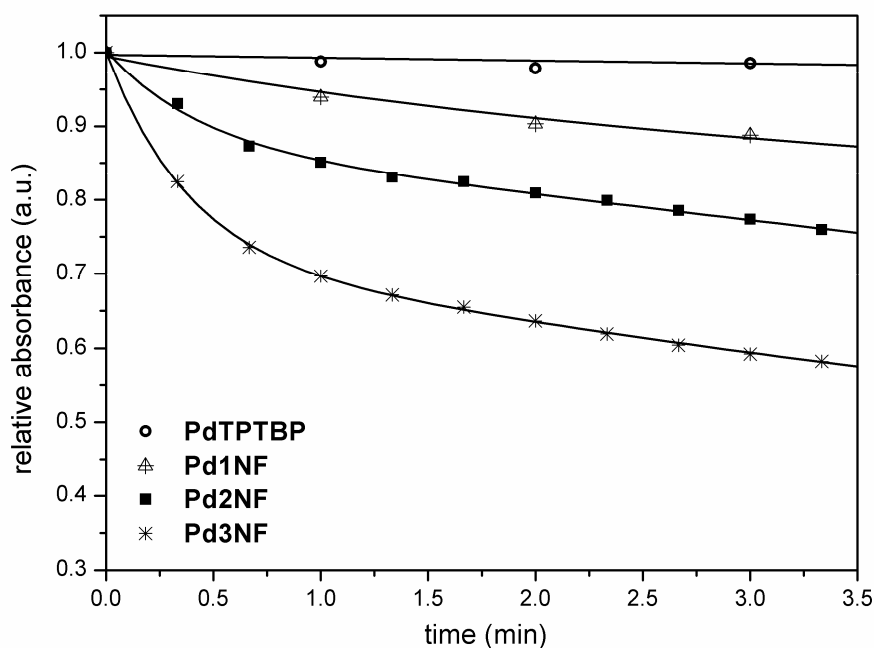


Figure S34. Photo-degradation curves for the palladium complexes in DMF solution at room temperature. Irradiation is performed with red LED array at 638 nm (flux: $6200 \mu\text{mols}^{-1}\text{m}^{-2}\mu\text{A}$).

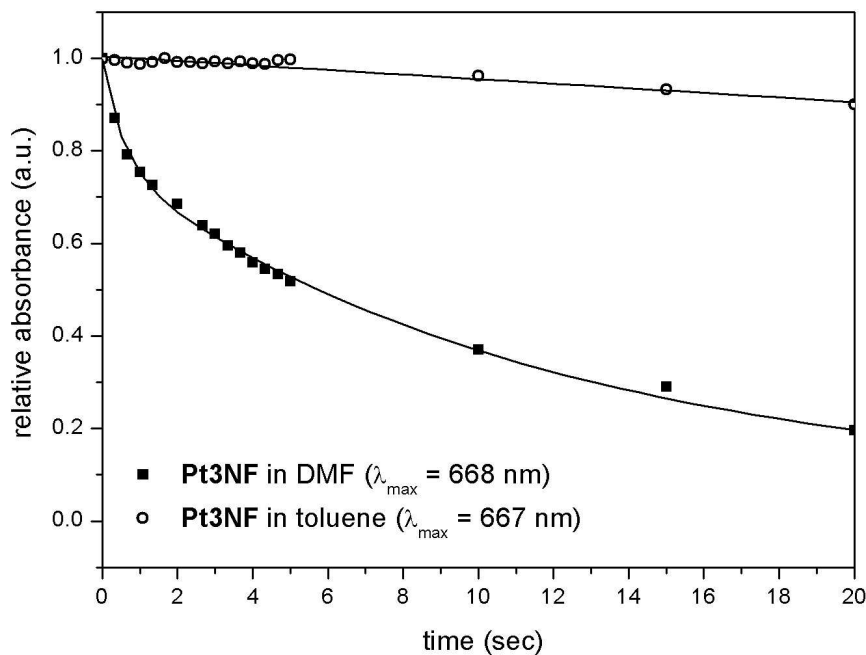


Figure S35. Photo-degradation curves for the platinum complex **Pt3NF** in DMF as well as in toluene solution at room temperature. Irradiation is performed with red LED array at 638 nm (flux: $6200 \mu\text{mols}^{-1}\text{m}^{-2}\mu\text{A}$).

MALDI-TOF

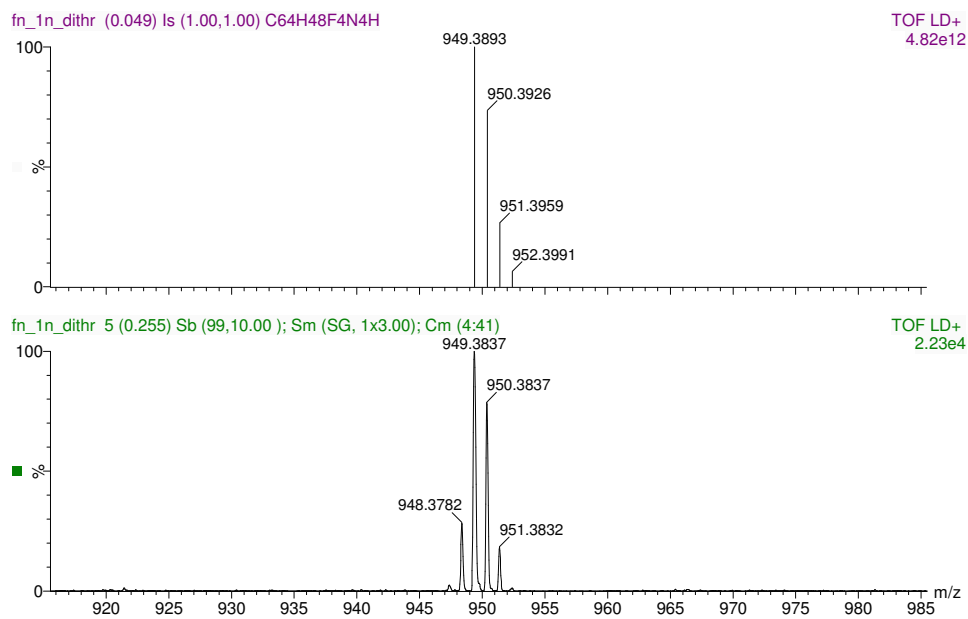


Figure S36. Calculated (above) and measured (below) isotope pattern of **1NF**.

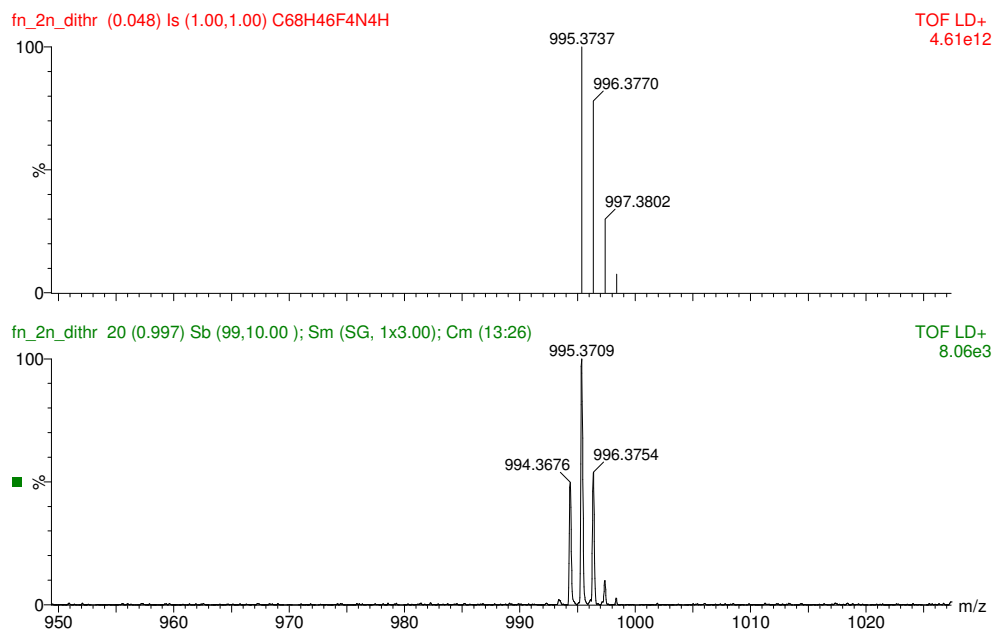


Figure S37. Calculated (above) and measured (below) isotope pattern of **2NF**.

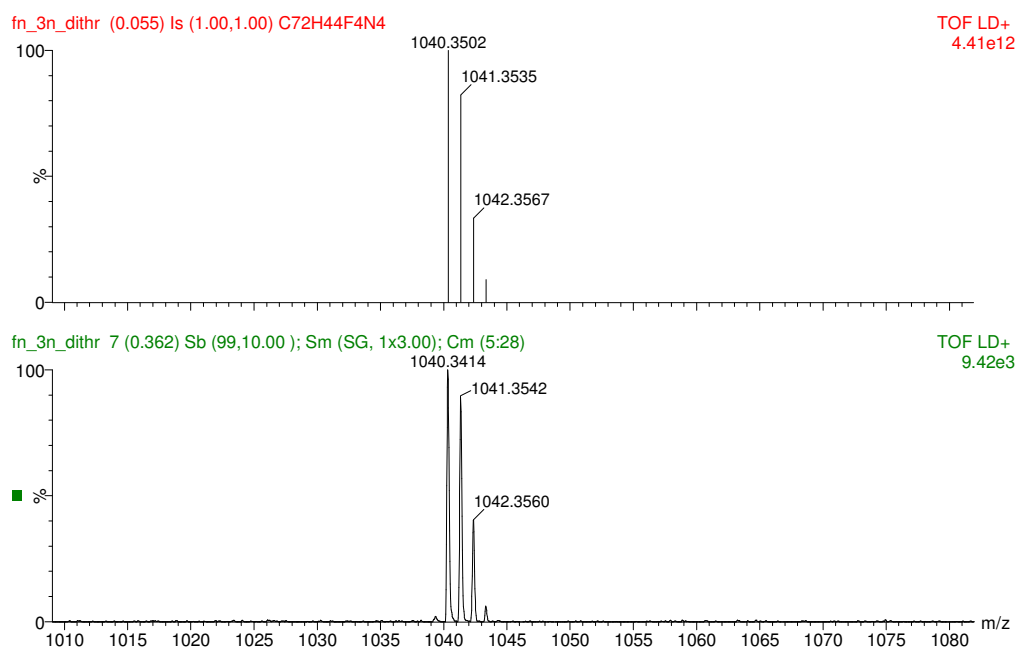


Figure S38. Calculated (above) and measured (below) isotope pattern of **3NF**.

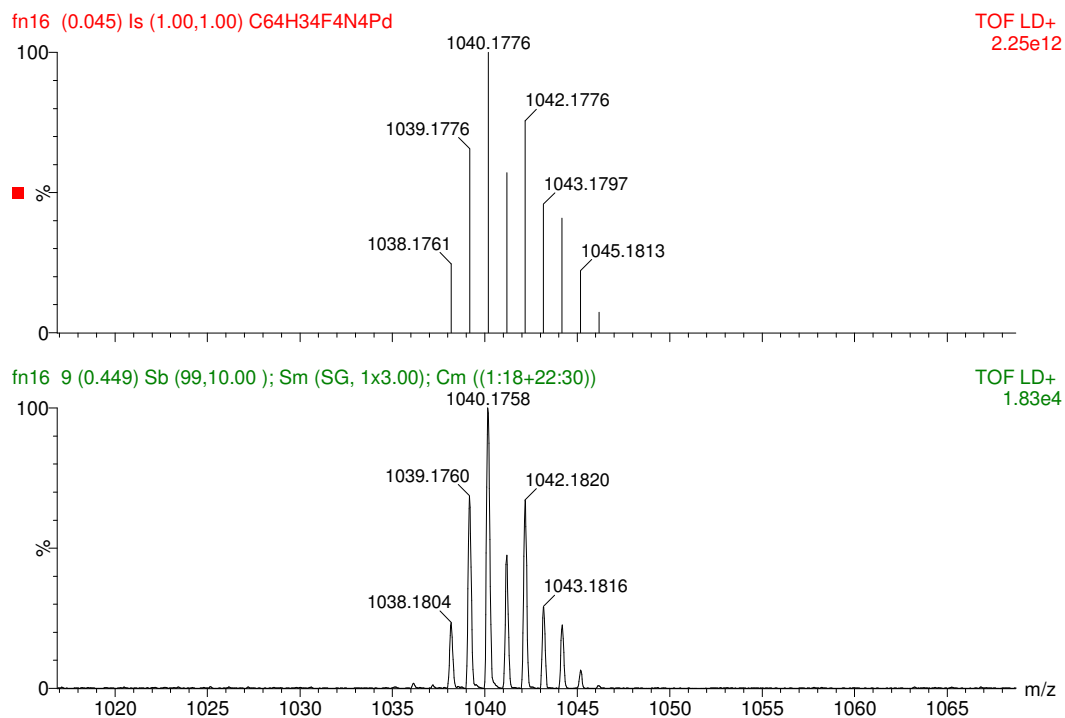


Figure S39. Calculated (above) and measured (below) isotope pattern of **Pd1NF**.

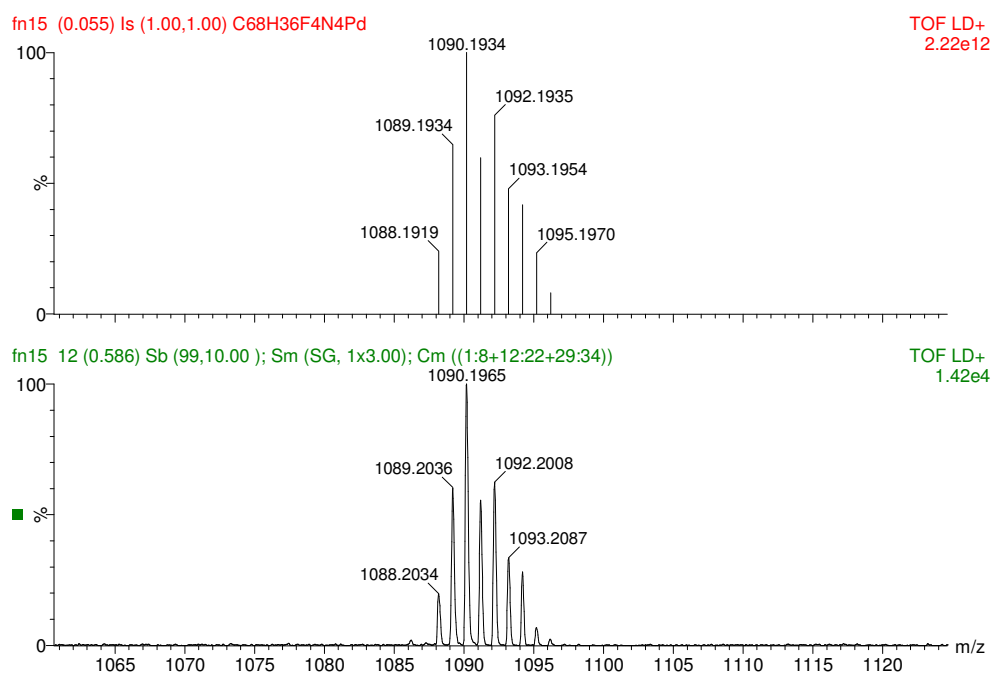


Figure S40. Calculated (above) and measured (below) isotope pattern of **Pd2NF**.

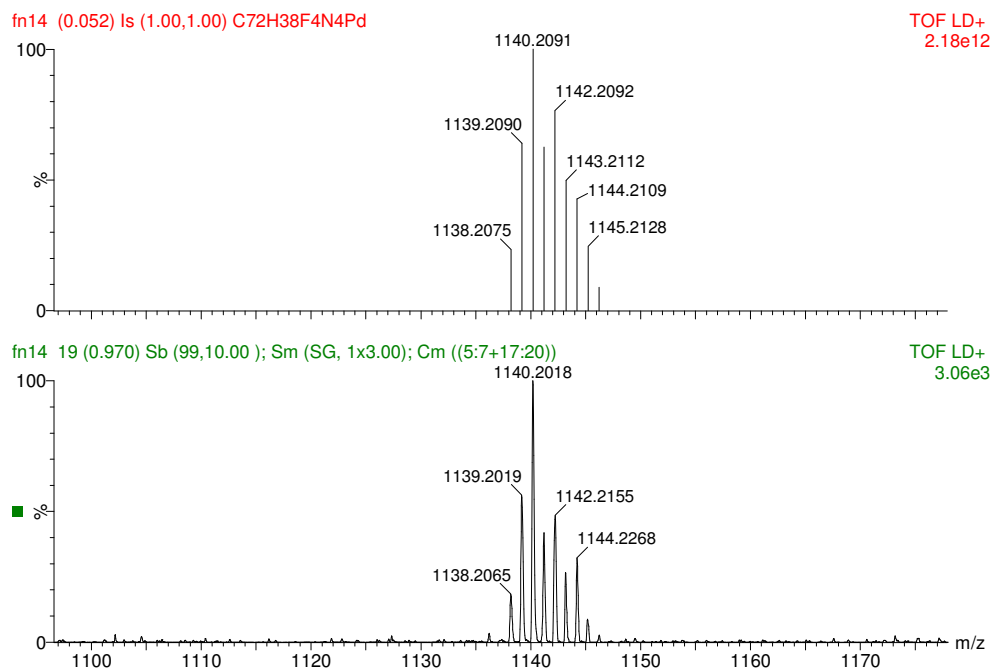


Figure S41. Calculated (above) and measured (below) isotope pattern of **Pd3NF**.

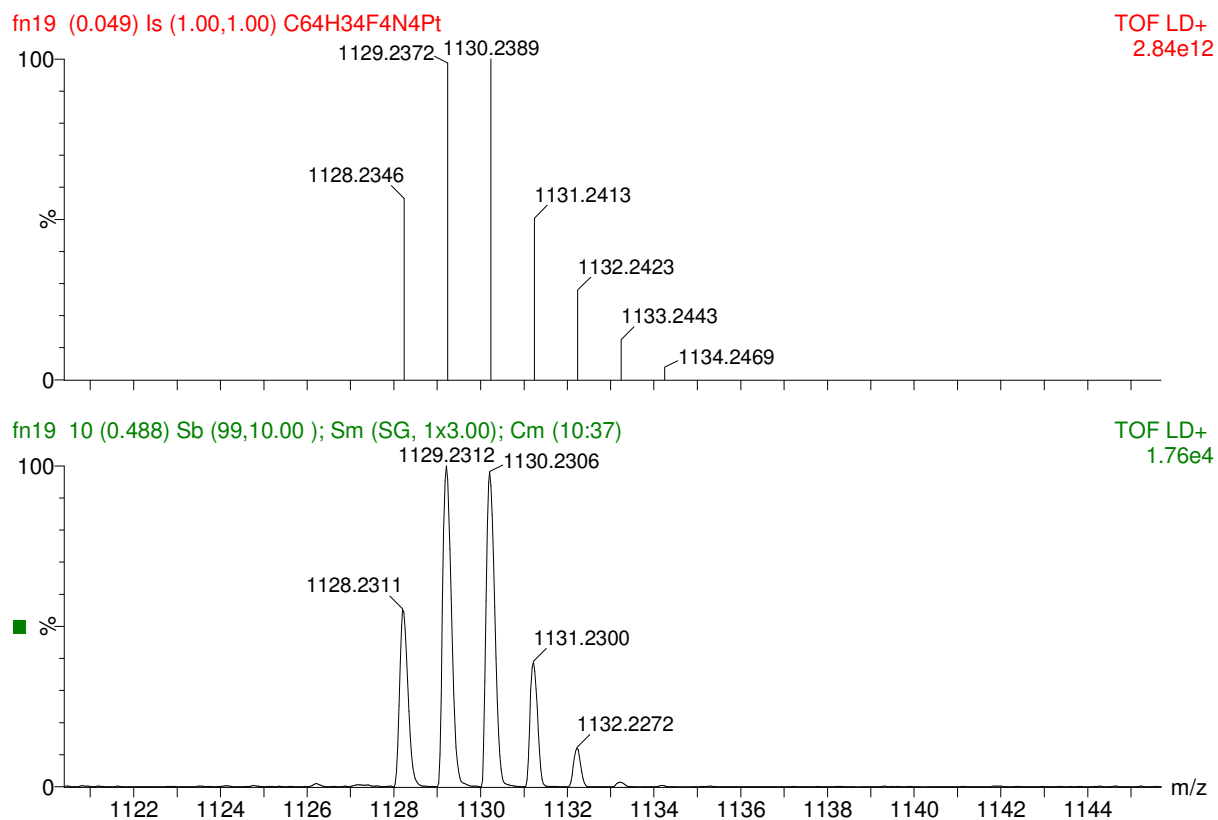


Figure S42. Calculated (above) and measured (below) isotope pattern of **Pt1NF**.

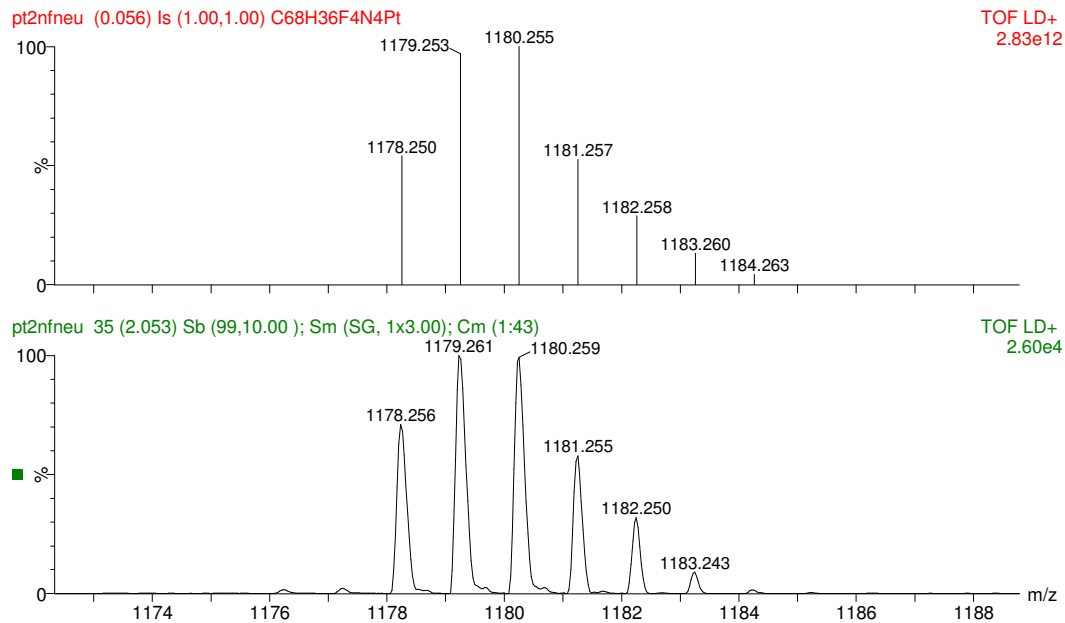


Figure S43. Calculated (above) and measured (below) isotope pattern of **Pt₂NF**.

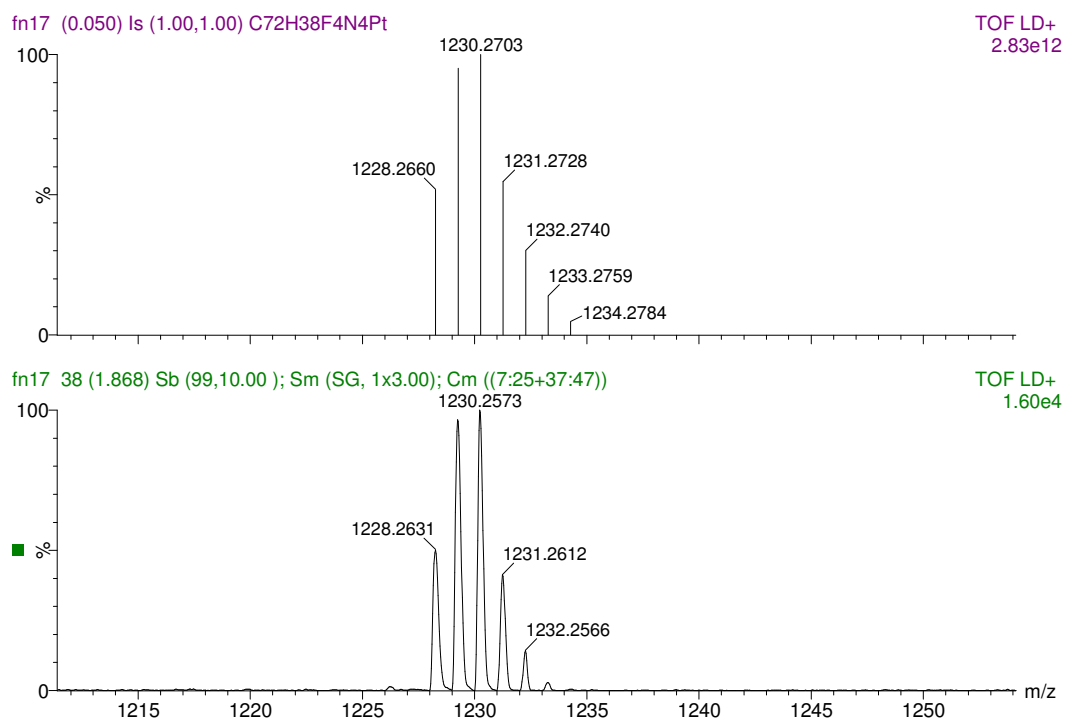


Figure S44. Calculated (above) and measured (below) isotope pattern of **Pt₃NF**.

DFT Calculations

Geometries

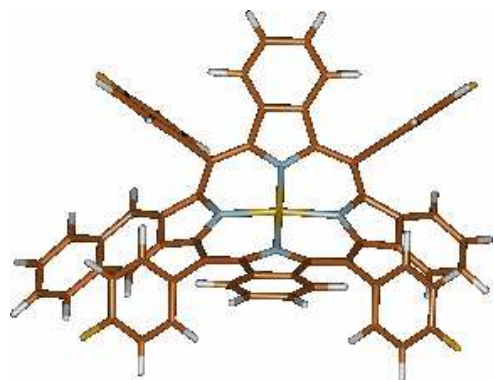


Figure S45. DFT optimized equilibrium geometry of **Pt1NF**.

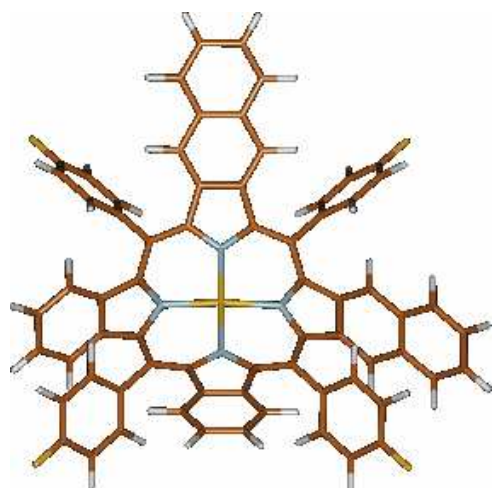


Figure S46. DFT optimized equilibrium geometry of *cis*-**Pt2NF**.

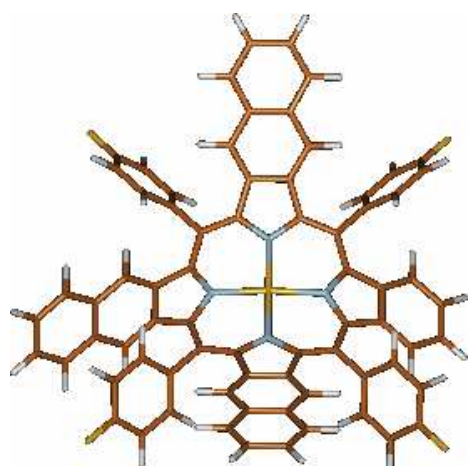


Figure S47. DFT optimized equilibrium geometry of **Pt3NF**.

Orbitals

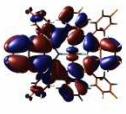
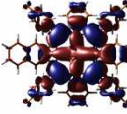
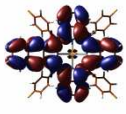
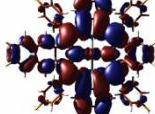
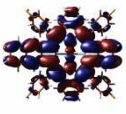
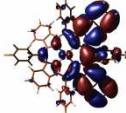
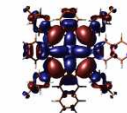
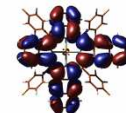
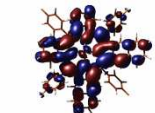
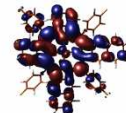
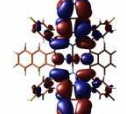
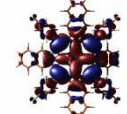
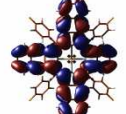
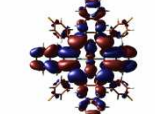

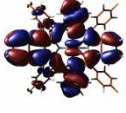
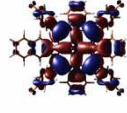
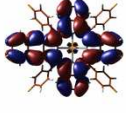
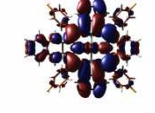
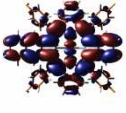
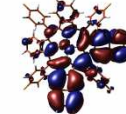
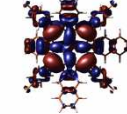
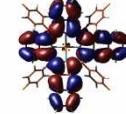
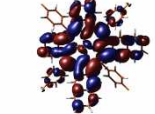
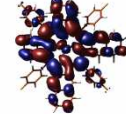
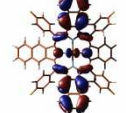
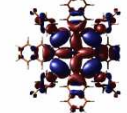

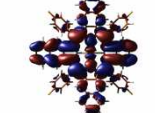
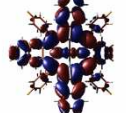
	HOMO-2	HOMO-1	HOMO	LUMO	LUMO+1
Pd1NF	 -5.92 eV	 -5.47 eV	 -4.80 eV	 -2.42 eV	 -2.34 eV
Pd2NF	 -5.83 eV	 -5.49 eV	 -4.71 eV	 -2.38 eV	 -2.38 eV
Pd3NF	 -5.77 eV	 -5.49 eV	 -4.63 eV	 -2.41 eV	 -2.33 eV
Pt1NF	 -5.89 eV	 -5.55 eV	 -4.82 eV	 -2.40 eV	 -2.32 eV
Pt2NF	 -5.81 eV	 -5.56 eV	 -4.73 eV	 -2.36 eV	 -2.36 eV
Pt3NF	 -5.75 eV	 -5.57 eV	 -4.65 eV	 -2.39 eV	 -2.32 eV

Figure S48. Energies and isodensity representations of the Kohn-Sham orbitals HOMO-2, HOMO-1, HOMO, LUMO, and LUMO+1 calculated for the title compounds.

References

- (1) Borek, C.; Hanson, K.; Djurovich, P.I.; Thompson, M.E.; Aznavour, K.; Bau, R.; Sun, Y.; Forrest, S.R.; Brooks, J.; Michalski, L.; Brown, J. *Angew. Chem. Int. Ed.* **2007**, *46*, 1109-1112.
- (2) Finikova, O. S.; Aleshchenkov, S. E.; Briñas, R. P.; Cheprakov, A. V.; Carroll, P. J.; Vinogradov, S. A. *J. Org. Chem.* **2005**, *70*, 4617-4628.
- (3) Menzek, A.; Altundas, A.; Gültekin, D. *J. Chem. Research (S)* **2003**, 752-753.
- (4) Perez, M. D.; Borek, C.; Forrest, S. R.; Thompson, M. E. *J. Am. Chem. Soc.* **2009**, *131*, 9281-9286.
- (5) Carraway, E. R.; Demas, J. N.; DeGraff, B. A.; Bacon, J. R. *Anal. Chem.* **1991**, *63*, 337-342.